

2017

Changes In Threonyl-Trna Synthetase Expression And Secretion In Response To Endoplasmic Reticulum Stress By Monensin In Ovarian Cancer Cells

Jared Louis Hammer
University of Vermont

Follow this and additional works at: <https://scholarworks.uvm.edu/graddis>

 Part of the [Biochemistry Commons](#), [Cell Biology Commons](#), and the [Pharmacology Commons](#)

Recommended Citation

Hammer, Jared Louis, "Changes In Threonyl-Trna Synthetase Expression And Secretion In Response To Endoplasmic Reticulum Stress By Monensin In Ovarian Cancer Cells" (2017). *Graduate College Dissertations and Theses*. 764.
<https://scholarworks.uvm.edu/graddis/764>

This Thesis is brought to you for free and open access by the Dissertations and Theses at ScholarWorks @ UVM. It has been accepted for inclusion in Graduate College Dissertations and Theses by an authorized administrator of ScholarWorks @ UVM. For more information, please contact donna.omalley@uvm.edu.

CHANGES IN THREONYL-TRNA SYNTHETASE EXPRESSION AND SECRETION
IN RESPONSE TO ENDOPLASMIC RETICULUM STRESS BY MONENSIN IN
OVARIAN CANCER CELLS

A Thesis Presented

by

Jared L. Hammer

to

The Faculty of the Graduate College

of

The University of Vermont

In Partial Fulfillment of the Requirements
for the Degree of Master of Science
Specializing in Biochemistry

October, 2017

Defense Date: May 17, 2017
Thesis Examination Committee:

Christopher S. Francklyn, Ph. D., Advisor
Dwight E. Matthews, Ph. D., Chairperson
Karen M. Lounsbury, Ph. D.
Robert J. Hondal, Ph. D.
Cynthia J. Forehand, Ph.D., Dean of the Graduate College

ABSTRACT

Aminoacyl-tRNA synthetases (ARS) are a family of enzymes that catalyze the charging of amino acids to their cognate tRNA in an aminoacylation reaction. Many members of this family have been found to have secondary functions independent of their primary aminoacylation function. Threonyl-tRNA synthetase (TARS), the ARS responsible for charging tRNA with threonine, is secreted from endothelial cells in response to both vascular endothelial growth factor (VEGF) and tumor necrosis factor- α (TNF- α), and stimulates angiogenesis and cell migration. Here we show a novel experimental approach for studying TARS secretion, and for observing the role of intracellular TARS in the endoplasmic reticulum (ER) stress response and in angiogenesis.

Using Western blotting, immunofluorescence microscopy and RT-qPCR we were able to investigate changes in TARS protein and transcript levels. We initially hypothesized that TARS was secreted by exosomal release, and so we treated a human ovarian cancer cell line (CaOV-3) with monensin, an ionophore that increases exosome production, and VEGF to observe changes in intracellular and extracellular TARS protein. Monensin treatment consistently increased extracellular and intracellular TARS protein, however CD63, an exosome marker protein, levels were unaffected by monensin treatment. VEGF had no effect on intracellular TARS. We therefore hypothesized that the TARS response was a result of ER stress.

The unfolded protein response (UPR) is a series of signaling pathways that are activated upon ER stress. When CaOV-3 cells were treated with increasing concentrations of monensin, intracellular levels of TARS and p-eIF2 α , a downstream UPR target, increased accordingly. Monensin increased intracellular TARS protein and transcript levels in CaOV-3 cells. Monensin also increased DNAJB9, an ER chaperone protein, transcript levels, further confirming ER stress. Interestingly, monensin increased VEGF transcript levels about 6-fold. Borrelidin, a natural TARS inhibitor, also increased VEGF transcript levels, and caused an increase in p-eIF2 α protein.

Although the mechanism of TARS secretion remains unresolved, these data indicate that intracellular TARS expression increases in response to ER stress by monensin. Given TARS and VEGF transcript expression increased accordingly, it is possible that intracellular TARS may have pro-angiogenic function. Future directions may include investigating TARS interactions with translational control machinery.

DEDICATION

I would like to dedicate this work to my parents, David and Audrey Hammer, for their endless love, their unwavering encouragement, and for believing in me wholeheartedly in all of my endeavors.

I would also like to dedicate this work to my dear, late friend Mary Wilk whose intelligence, love and cheer inspired me daily throughout this project.

ACKNOWLEDGEMENTS

Dr. Francklyn, thank you for your support and guidance over the past two years. I am fortunate to have had the opportunity to work with such a curious and passionate scientist who truly cares about the success of his students. You have taught me how to look at problems critically, how to question results and think deliberately, and have pushed me to be a better problem solver. You inspire me to continue to pursue science in the future.

Dr. Lounsbury, your commitment to my learning and success is more than I could have hoped for. Your insight and technical advice have been invaluable. Thank you for teaching me laboratory skills, for your willingness to talk through complex topics, and for indirectly taking on the role as my second advisor. You inspire me to be a better scientist, and to pursue my passion.

Terry, Dr. Jamie Abbott and Dr. Susan Robey-Bond, without your guidance and knowledge I do not see how I could have completed this thesis. Thank you for your support and curiosity. It was a pleasure to work with you and all other members of the Francklyn and Lounsbury labs.

Thank you to my family and friends for the love and encouragement I have received over this past year. I could not have done it without you.

Thank you to my committee members, Drs. Robert Hondal and Dwight Matthews, for your insight into my project. Finally, special thanks to Dr. Alan Howe for letting me use his microscope, and to Drs. Jay Silveira and Stephen Everse who supported me as an undergraduate student at UVM and gave me the opportunity to participate in the Biochemistry AMP program.

TABLE OF CONTENTS

	Page
DEDICATION	ii
ACKNOWLEDGEMENTS	iii
LIST OF FIGURES	vi
LIST OF TABLES	vii
LIST OF ABBREVIATIONS	viii
CHAPTER 1: INTRODUCTION.....	1
1.1 Aminoacyl-tRNA Synthetase Primary Function	1
1.1.1 Aminoacyl-tRNA Synthetases are Vital for Translation.....	1
1.1.2 Maintaining Fidelity when Charging tRNA Molecules	3
1.2 Aminoacyl-tRNA Synthetases in Disease	6
1.2.1 Introduction to Synthetases in Disease.....	6
1.2.2 Neurodegeneration	7
1.2.3 Synthetases are Involved in Autoimmunity	9
1.2.4 Synthetase Effects on Tumor Progression.....	10
1.3 Angiogenesis	13
1.3.1 Angiogenesis Background.....	13
1.3.2 Synthetase Angiogenic Activity	15
1.3.3 Possible Mechanisms of Synthetase Secretion.....	17
1.4 Endoplasmic Reticulum Stress Response.....	19
1.4.1 Endoplasmic Reticulum Stress and the Unfolded Protein Response.....	19
1.4.2 General Control Nonderepressible 2	22
1.4.3 Synthetase Involvement in ER Stress.....	23
1.4.4 Monensin	24
1.5 Experimental Model	25

CHAPTER 2: EXPERIMENTAL PROCEDURES AND MATERIALS.....	26
CHAPTER 3: EXTRACELLULAR TARS PROTEIN LEVELS INCREASE IN CAOV-3 CELLS IN REPSONSE TO MONENSIN TREATMENT WHILE CD63 PROTEIN IS UNAFFECTED.....	33
3.1 Introduction	33
3.2 Results	33
CHAPTER 4: INTRACELLULAR TARS LEVELS IN CAOV-3 CELLS ARE AFFECTED BY MONENSIN TREATMENT	38
4.1 Introduction	38
4.2 Results	38
4.3 Conclusion.....	55
CHAPTER 5: DISCUSSION AND FUTURE DIRECTIONS	56
5.1 Monensin as a Novel Model to Study TARS	56
5.1.1 Molecular Effects of Monensin	56
5.1.2 Exosomal Detection.....	57
5.2 Post-translational Modifications.....	59
5.2.1 Palmitoylation.....	59
5.2.2 The Ubiquitin Family of Modifications	60
5.3 Integration of Eukaryotic Translation, ER Stress and Hypoxia	63
5.3.1 Hypoxic Translation Machinery	63
5.3.2 Does TARS Interact with Hypoxic Translation Machinery in Cancer Cells?.....	64
5.3.3 Comparison of Monensin and Borrelidin Effects on TARS	67
5.4 Final Remarks.....	69
CHAPTER 6: BIBLIOGRAPHY	71
CHAPTER 7: APPENDIX.....	83

LIST OF FIGURES

	Page
Fig. 1: Mechanism of increased VEGF translation by $\alpha 6\beta 4$ integrin activation	14
Fig. 2: Proposed mechanism of exosome formation and subsequent release.....	18
Fig. 3: Diagram of UPR signaling pathways.....	21
Fig. 4: TARS is secreted out of CaOV-3 cells in response to monensin treatment	34
Fig. 5: TARS protein secretion increases with monensin and VEGF cell treatments while CD63 is unaffected	36
Fig. 6: Monensin and VEGF treatments of CaOV-3 cells do not affect intracellular CD63 protein levels.....	37
Fig. 7: TARS protein increases intracellularly in response to monensin by Western blot.....	39
Fig. 8: Monensin-treated CaOV-3 cells have increased intracellular TARS by IMF microscopy	42
Fig. 9: TARS localizes to the cytoplasm of CaOV-3 cells.....	43
Fig. 10: Changing mRNA expression levels in CaOV-3 cells in response to ER stress...	45
Fig. 11: TARS and p-eIF2 α protein levels increase in response to increasing monensin.....	47
Fig. 12: TARS and VEGF transcript levels increase in response to increasing monensin.....	50
Fig. 13: Borrelidin treatment causes p-eIF2 α protein to increase but not TARS protein..	53
Fig. 14: Transcript levels increase in response to borrelidin and monensin treatments....	54
Fig. 15: Structures of MG132, Monensin and Borrelidin	62
Fig. 16: TARS interacts with members of the hypoxic translation machinery complex independent of hypoxia	66
Fig. 17: Summary of effects of monensin and borrelidin on ER stress and integration with hypoxic translation	69

LIST OF TABLES

	Page
Table A.1: NanoSight particle analysis of exosome-precipitated samples from CaOV-3 cells	83

LIST OF ABBREVIATIONS

4EBP – 4E-binding protein
AA – Amino acid
AARS – Alanyl-tRNA synthetase
AIMP – ARS-interacting multifunctional protein
Akt – Protein kinase B
ARS – Aminoacyl-tRNA synthetase
ATF4 – Activating transcription factor 4
ATF6 – Activating transcription factor 6
ATP – Adenosine triphosphate
BiP – Binding immunoglobulin protein
CAM – Chorioallantoic membrane assay
CHOP – C/EBP homologous protein
CREB – cAMP response element-binding protein
DAPI – 4'-6-Diamidine-2'-phenylindole dihydrochloride
DARS – Aspartyl-tRNA synthetase
DMSO – Dimethyl sulfoxide
eIF2 α – Eukaryotic translation initiation factor-2 α
eIF4E – Eukaryotic translation initiation factor-4E
eIF4E2 – Eukaryotic translation initiation factor-4E2
eNOS – Nitric oxide synthase
EPRS – Glutamyl-prolyl-tRNA synthetase
ER – Endoplasmic reticulum
ERK – Extracellular-signal-regulated kinase
FARS – Phenylalanyl-tRNA synthetase
FBS – Fetal bovine serum
GAIT – Gamma interferon inhibitor of translation
GARS – Glycyl-tRNA synthetase
GCN2 – General control nonderepressible 2
HARS – Histidyl-tRNA synthetase
Hif – Hypoxia inducible factor
IARS – Isoleucyl-tRNA synthetase
IFN – Interferon- λ
IP – Immunoprecipitate
IRE1- α – Inositol-requiring enzyme 1
KARS – Lysyl-tRNA synthetase
LARS – Leucyl-tRNA synthetase
MARS – Methionyl-tRNA synthetase
MSC – Multi synthetase complex
PERK – PRKR-like ER kinase
PI3-K – Phosphoinositide-3 kinase
PMN – Polymorphonuclear leukocyte
PTM – Post-translational modification

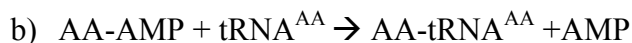
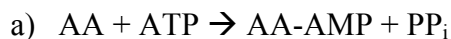
QARS – Glutaminyl-tRNA synthetase
RARS – Arginyl-tRNA synthetase
RBM4 – Ribosome-binding protein 4
SARS – Seryl-tRNA synthetase
TARS – Threonyl-tRNA synthetase
TNF- α – Tumor necrosis factor- α
TRAF-2 – TNF receptor associated factor-2
tRNA – transfer Ribonucleic acid
UPR – Unfolded protein response
VARS – Valyl-tRNA synthetase
VEGF – Vascular endothelial growth factor
WARS – Tryptophanyl-tRNA synthetase
XPB1 – X-box binding protein 1
YARS – Tyrosyl-tRNA synthetase

CHAPTER 1: INTRODUCTION

1.1 Aminoacyl-tRNA Synthetase Primary Function

1.1.1 Aminoacyl-tRNA Synthetases are Vital for Translation

Aminoacyl-tRNA synthetases (ARSs) are responsible for charging transfer ribonucleic acid (tRNA) molecules with their cognate amino acids via an aminoacylation reaction. ARSs were first discovered by their ability to activate amino acids and transfer those amino acids to tRNA in the presence of microsomal RNA fractions from rat liver and adenosine triphosphate (ATP) (Zamecnik and Keller 1954, Hoagland, Stephenson et al. 1958). ARSs are evolutionarily conserved across kingdoms, as this reaction is necessary for global translation (Szymanski, Deniziak et al. 2001). In order to ensure amino acid fidelity when charging tRNA molecules each tRNA species has a subsequent ARS, with some exceptions (Ibba, Becker et al. 2000). The following highlights the two-step reaction ARSs catalyze:



In part (a) of this reaction, the synthetase reacts its cognate amino acid (AA) with a molecule of ATP to produce an adenylate intermediate (AA-AMP) and inorganic phosphate (PP_i). AA-AMP remains bound in the active site of the enzyme. The corresponding tRNA ($tRNA^{AA}$) then enters the active site, and the amino acid's carboxyl group binds to either the 2' or 3'-OH of the 3' end of the tRNA thus transferring from the ARS to the tRNA. The charged tRNA is then released from the ARS and can be recruited

for translation. This model suggests that these are two separate reactions where in reality there is coupling between the two reactions, which is vital for proper ARS function. This reaction comprises the primary function of all ARSs.

ARSs can be categorized into two different classes. Class I synthetases have a Rossmann fold, a parallel β -sheet, located in their active site, and bind tRNA in the minor groove of the acceptor stem where they aminoacylate on the tRNA 2'-OH (Ibba, Becker et al. 2000). Class I synthetases also share the sequence motifs HIGH and KMSKS, and are typically monomeric when active (Arnez and Moras 1997). In contrast, class II synthetases have an antiparallel β -sheet in their active site, which is surrounded by α -helices, and bind tRNA in the major groove of the acceptor stem where the 3'-OH is aminoacylated (Arnez and Moras 1997, Ibba, Becker et al. 2000). This class of synthetases typically exists as a dimer or multimer upon catalytic activation. Class II synthetases share sequence motifs, referred to as motifs 1, 2 and 3, which are structurally vital for enzyme function. Motif 1 consists of an α -helix linked to a β -strand, and is located at the dimer interface of class II ARSs, while motifs 2 and 3 are found in the active site of the enzyme, and consist of two anti-parallel β -strands linked by a loop and a β -strand followed immediately by an α -helix, respectively (Arnez and Moras 1997). Two exceptions to these parameters are lysyl-tRNA synthetase (KARS), which is both a class I and class II synthetase, and phenylalanyl-tRNA synthetase (FARS), which is a class II synthetase that aminoacylates on the 2'-OH of tRNA (Ibba, Becker et al. 2000).

1.1.2 Maintaining Fidelity When Charging tRNA Molecules

ARSs are vital for proper protein synthesis, and so they must have a high rate of fidelity for aminoacylating tRNA molecules with their cognate amino acids. ARSs must distinguish correct tRNA and amino acid molecules to ensure the correct tRNA molecules are charged with their cognate amino acids. This process aims to combat mutations during translation. Cognate tRNA molecules are distinguished by interactions with specific nucleotides on the tRNA, known as identity elements (Giege, Sissler et al. 1998). This recognition has shown little error. It is reported that 1 in 10^7 misidentification events occur, which would not contribute greatly to overall translational error (Jakubowski and Goldman 1992). Incorporation of cognate amino acids into AA-tRNA^{AA} complexes requires a more complicated editing mechanism.

ARSs need to be able to distinguish between cognate and non-cognate amino acids with high fidelity in order to mitigate mutational errors in translation. Some amino acids are structurally similar, and cannot be easily distinguished by ARSs. For example, valine and isoleucine differ in structure by a single methyl group. The fidelity of synthetases is maintained by a two-step editing process known as the “double sieve model” (Sankaranarayanan and Moras 2001).

This enzyme hyperspecificity was first rationalized in 1976 by Fersht and Kaethner who showed a low rate of misincorporation of threonine onto tRNA^{Val} by valyl-tRNA synthetase (VARs) (Fersht and Kaethner 1976). They proposed a two-step model. First, cognate and near-cognate amino acids are filtered out from larger amino acids in the active site, and charged accordingly in an adenylation reaction. Second, mischarged amino acids are hydrolyzed to ensure misincorporation during translation does not occur.

For example, VARS will charge threonine and form a complex with a threonyl-adenylate at 1:1, however when a Thr-VARS-tRNA^{Val} complex forms, the aminoacylated product is rapidly hydrolyzed (Fersht and Kaethner 1976). The term double sieve model was coined for this process shortly thereafter (Fersht and Dingwall 1979).

Since then, the double sieve model has been further examined, and the original hypothesis by Fersht and Kaethner has been modified by crystal structure analysis and by monitoring acylation activity (Martinis and Boniecki 2010). The first step in editing consists of the “coarse sieve”, which refers to amino acids of similar size, cognate and non-cognate, binding in the active site of the ARS, while larger amino acids are typically excluded due to steric hindrance (Sankaranarayanan and Moras 2001). In the case of isoleucyl-tRNA synthetase (IARS), valine and isoleucine differ by only one methyl group, which translates to a difference of about 1 kcal/mol of binding energy difference (Nureki, Vassylyev et al. 1998). IARS therefore misincorporates valine for isoleucine at a rate of about one in five thus creating a thermodynamically unfavorable model for one-step discrimination (Nureki, Vassylyev et al. 1998). A second editing step has evolved to counter this high rate of misincorporation.

“Fine sieve” editing refers to hydrolysis of false cognates, and can be further categorized into pre-transfer and post-transfer editing. The pre-transfer mechanism involves hydrolysis of the false cognate adenylate intermediate, while the post-transfer mechanism involves deacylation of the incorrectly charged tRNA (Sankaranarayanan and Moras 2001). IARS primarily employs pre-transfer editing. Valyl-adenylate intermediates are hydrolyzed in the presence of tRNA^{Ile} while isoleucyl intermediates are successfully transferred to tRNA^{Ile} as demonstrated in *E. coli* and *T. thermophilus* (Baldwin and Berg

1966, Nureki, Vassilyev et al. 1998). Post-transfer editing occurs in a second hydrolytic site separate from the active site (Martinis and Boniecki 2010). ARSs that employ this mechanism will charge tRNA with non-cognate adenylate intermediates, and then transfer the complex to the hydrolytic site. tRNA molecules charged with cognate amino acids do not fit in this site and are released. Pre- and post-transfer mechanisms are sometimes both present in the same ARS, suggesting redundancy in editing (Martinis and Boniecki 2010).

Class I synthetases have a conserved CP1 domain in their active site, which is employed for editing non-cognate substrates (Marintchev 2012). In contrast class II synthetases vary in their structural organization resulting in specific motifs that create variance in editing mechanisms across ARSs (Marintchev 2012). One of the most well understood mechanisms of class II synthetase editing is that of threonyl-tRNA synthetase (TARS).

TARS has a molecular weight of 83 kiloDaltons and dimerizes to gain catalytic activity. During editing, TARS has to distinguish between threonine, serine and valine when charging tRNA^{Thr} molecules. Valine is isosteric with threonine, the cognate substrate, and serine differs from threonine by one methyl group. TARS has a zinc ion in its active site, which is coordinated by three residues and a water molecule (Marintchev 2012). This zinc ion acts as a cofactor in amino acid recognition, interacting with the hydroxyl side chains of threonine and serine (Sankaranarayanan and Moras 2001). Therefore, valine is entirely excluded by TARS due to its lack of a hydroxyl group (Marintchev 2012). TARS then uses its N-terminal N2 domain to employ a post-transfer editing mechanism to hydrolyze Ser-tRNA^{Thr} complexes (Dock-Bregeon,

Sankaranarayanan et al. 2000, Sankaranarayanan and Moras 2001, Marintchev 2012). TARS utilizes a chemical “coarse sieve” following by a more traditional post-transfer “fine sieve” when discriminating between cognate and non-cognate amino acids.

1.2 Aminoacyl-tRNA Synthetases in Disease

1.2.1 Introduction to Synthetases in Disease

Proper ARS function, including fidelity in aminoacylation, is not only important for maintaining translation integrity, but also for preventing disease. Mutations in ARSs play a role in pathology, as these mutations often inhibit tRNA aminoacylation and disrupt protein synthesis (Yao and Fox 2013, Abbott, Francklyn et al. 2014). Synthetase dysfunction has been linked with neurodegenerative disorders, angiogenesis, tumorigenesis and inflammation (Yao and Fox 2013, Abbott, Francklyn et al. 2014). It has been reported in mice that a missense mutation in the editing domain of alanyl-tRNA synthetase (AARS) causes cerebellar Purkinje cell loss and ataxia showing direct correlation with loss of editing function and disease (Lee, Beebe et al. 2006). In contrast, Charcot-Marie-Tooth disease (CMT) has been linked with mutations in KARS, glycyl-tRNA synthetase (GARS), AARS, tyrosyl-tRNA synthetase (YARS) and histidyl-tRNA synthetase (HARS) that do not lead to loss of editing function (Yao and Fox 2013, Abbott, Francklyn et al. 2014). ARSs’ roles in various diseases have yielded insight into secondary functions of this family of enzymes.

Synthetases and their associated factors are well established in the roles they play in diseases. Specifically, these molecules contribute to neurodegenerative disorders,

autoimmune disorders and cancer progression. This has rendered many members of the ARS family valid targets for pharmacological intervention.

1.2.2 Neurodegeneration

The majority of the 20 standard amino acids have two synthetases associated with them, a cytoplasmic and mitochondrial species (Kurland and Andersson 2000).

Mitochondrial synthetases play a role in synthesis of components of the mitochondrial oxidative phosphorylation system, while cytoplasmic synthetases are involved in more global protein synthesis (Konovalova and Tyynismaa 2013). As a result, there are diseases associated with synthetases of both mitochondrial and cytoplasmic ARSs.

Mitochondrial tRNA and mitochondrial ARS mutations contribute to many neurodegenerative diseases. Briefly, the mitochondrial genome encodes for all RNA necessary for translation in the mitochondria, however proteins necessary for protein synthesis in the mitochondria, such as ARSs, ribosomal proteins etc., are encoded for in the nucleus, and are synthesized in the cytoplasm and transported into the mitochondria (Abbott, Francklyn et al. 2014). Mitochondrial tRNA mutations accumulate over the course of an organism's life cycle, and ultimately manifest in disease (Abbott, Francklyn et al. 2014). Two well characterized diseases resulting from this accumulation are mitochondrial encephalomyopathy, lactic acidosis, and stroke-like episodes (MELAS) and myoclonic epilepsy with ragged red fibers (MERRF) (Abbott, Francklyn et al. 2014). These diseases can lead to symptoms including epilepsy, seizures and limb weakness. 80% of MELAS patients contain an A3243G mutation in the tRNA^{Leu} gene, while 80-90% of MERRF patients exhibit an A8344G mutation in the tRNA^{Lys} gene (Silvestri,

Moraes et al. 1992, Suzuki, Nagao et al. 2011). MELAS mutations lead to impaired oxidative phosphorylation due to defects in respiratory chain complexes I and IV (Abbott, Francklyn et al. 2014). In addition, in both MELAS and MERFF patients a G12147A mutation was found in tRNA^{His}, which was linked with a decrease in cytochrome c oxidase by succinate dehydrogenase staining and a decrease in mitochondrial protein synthesis (Melone, Tessa et al. 2004). These diseases highlight how mitochondrial tRNA mutations lead to dysfunctional mitochondria and subsequent modulation of brain function.

Mutated mitochondrial ARSs have also been linked with diseases of the brain. Leukoencephalopathy with brain stem and spinal cord involvement and lactate elevation (LBSL) is an autosomal recessive disorder that manifests in and contributes to changes in the white matter, which can lead to cerebellar ataxia, spasticity and dorsal column dysfunction (van Berge, Dooves et al. 2012, Konovalova and Tyynismaa 2013). LBSL is caused by mutations in the mitochondrial aspartyl-tRNA synthetase (DARS) gene with the most common mutation found in intron 2 across patients, which is important in the proper splicing of exon 3 (van Berge, Dooves et al. 2012). It was found that this mutation has the largest effect on exon 3 exclusion in patient neural cells compared with non-neural cells, and these neural cells also have more difficulty with correct inclusion of exon 3 than non-neural cells (van Berge, Dooves et al. 2012). This study not only links a mutated ARS with neurodegeneration, but also shows that these mutations are tissue specific. Tissue specificity is common in mitochondrial ARS and tRNA mutation phenotypes.

A common cytoplasmic ARS-associated disease is Charcot-Marie-Tooth syndrome (CMT). CMT is a neurodegenerative disease that is a result of peripheral neuropathy or degeneration of distal motor and sensory neurons. It ultimately leads to muscle weakness, altered gait and balance and general decline of leg and arm function. Six ARS mutations have been linked to CMT including AARS, GARS, HARS, KARS, methionyl-tRNA synthetase (MARS) and YARS (Yao and Fox 2013, Abbott, Francklyn et al. 2014). G41R, E196K and Δ 153-156 deletion mutations in YARS are linked with CMT (Jordanova, Irobi et al. 2006). Specifically, these mutations are associated with deteriorated canonical function of YARS, but this loss of function is not linked with CMT contribution (Jordanova, Irobi et al. 2006). YARS localizes to neuronal cells, and transfection with either wild type (WT) or mutant YARS into N2a cells shows no difference in localization patterns (Jordanova, Irobi et al. 2006). Therefore mutant YARS can be expected to affect neuronal cells. This is an example of how investigating synthetase mutants further may yield insight into neurodegeneration.

1.2.3 Synthetases are Involved in Autoimmunity

The ARS family is also associated with the autoimmune response. Autoimmunity refers to *in vivo* synthesis of antibodies against epitopes of non-foreign proteins, typically leading to protein dysfunction and subsequent disruption of cell health. Therefore, synthetases provide autoantigens that the body creates autoantibodies against, which intermittently sustains the autoimmune response. Myositis is an autoimmune disorder resulting in inflammation and weakness of muscle tissue. HARS and TARS both contain autoantigens associated with myositis (Miller, Waite et al. 1990, Williams, Miranda et al.

2013, Zhou, Wang et al. 2014). With respect to HARS, it has been well established that in myositis patients there are autoantibodies against HARS that are dependent on 3D enzyme structure and on tRNA^{His} binding in the active site of HARS (Miller, Waite et al. 1990, Zhou, Wang et al. 2014). HARS autoantibodies also undergo maturation to their target autoantigen, which solidifies the autoimmune response (Miller, Waite et al. 1990). TARS is the target of the autoantibody PL-7, and its targeting elicits a strong cytokine response, which has been associated with interstitial lung disease (Labirua and Lundberg 2010). The involvement of ARSs with autoimmune disorders furthers their validity for pharmacological targeting.

1.2.4 Synthetase Effects on Tumor Progression

When a cell becomes cancerous, various molecular and physiological events must occur in order to promote the proliferation and spread of the mutated cell. The accumulated mutations must be maintained throughout cell division, and the cancer cell must promote proper nutrient and growth factor recruitment in order to survive and spread. There is recent evidence supporting many members of the cytoplasmic ARS family being involved in progression of various tumors (Kim, You et al. 2011).

ARS involvement in tumor development has been widely categorized. Catalytically active MARS has been found to be elevated in colon cancer tissue (Kushner, Boll et al. 1976). This suggests that the tumor microenvironment may be trying to increase its total protein synthesis. Of note, MARS transcript was found to share a 55 base pair sequence homology with C/EBP homologous protein (CHOP) transcript, overlapping in their 3' UTR regions, which allows the two mRNAs to interact *in vivo*

(Ubeda, Schmitt-Ney et al. 1999). CHOP is typically a regulator of the unfolded protein response, however it has been found to be amplified in various cancers (Forus, Florenes et al. 1994). The interaction between the two transcripts promotes stability, and although this link has not been clearly linked with tumor progression, there is evidence supporting the possibility (Ubeda, Schmitt-Ney et al. 1999). In addition to its transcriptional interaction with CHOP, MARS is also a part of the multi synthetase complex (MSC), which serves as an integrating point for non-canonical ARS activity involved in tumorigenesis (Kim, You et al. 2011).

The MSC consists of D-, glutamyl-prolyl (EP)-, I-, K-, leucyl (L)-, M-, glutaminyl (Q)- and arginyl (R)-tRNA synthetases, and it interacts with three auxiliary cofactors, ARS-interacting multifunctional protein-1 (AIMP-1), AIMP-2 and AIMP-3 (Ray, Arif et al. 2007). AIMP-1, AIMP-2 and AIMP-3 interact with RARS, KARS and MARS, respectively. These multifunctional proteins are intricately interwoven with tumor regulatory pathways. Upon DNA mutation, AIMP-2 is phosphorylated leading to its dissociation from the MSC (Han, Park et al. 2008). AIMP-2 then binds and activates p53 protein, which inhibits binding of mouse double minute 2 homolog (MDM2) and subsequent ubiquitinylation and degradation of p53 (Han, Park et al. 2008). AIMP-2 has also been found to increase HEK293 cell's sensitivity to tumor necrosis factor- α (TNF- α) induced apoptosis by targeting TNF receptor associated factor 2 (TRAF2) for ubiquitinylation and degradation (Choi, Kim et al. 2009). This exemplifies the close interaction the MSC has with tumor regulatory pathways, and raises question as to what may occur if the complex were misregulated or mutated.

ARS protein expression in cancer cells themselves yields insight into possible roles different synthetases play in cancer. In SKOV-3 cells, an ovarian cancer cell line, TARS is secreted in response to TNF- α , similarly to endothelial cells (Williams, Mirando et al. 2013, Wellman, Eckenstein et al. 2014). TARS is overexpressed in ovarian carcinoma cells, and TARS concentration in these cells increases as tumor stage increases (Wellman, Eckenstein et al. 2014). Finally, TARS was found to coexpress with VEGF by immunohistochemistry in infiltrating leukocytes in ovarian cancer tumors (Wellman, Eckenstein et al. 2014). Taken together, these data propose ovarian cancer cells as a valid *in vitro* model for studying TARS expression as it relates to cancer.

In contrast, tryptophanyl-tRNA synthetase (WARS) has low expression levels in colorectal cancer (Ghanipour, Jirstrom et al. 2009). Low WARS expression was correlated with an increased risk of lymph node metastasis, and a lower survival rate than patients with increased WARS expression in cancer cells (Ghanipour, Jirstrom et al. 2009). WARS is anti-angiogenic, and so its decreased expression in colorectal cancer cells is likely acting as a protective mechanism to enable the tumor cell to increase its ability to promote angiogenesis (Tzima and Schimmel 2006). The difference in expression levels of different ARSs in cancer cells shows that the role of synthetases expands beyond increasing protein translation in tumor cells.

ARSs have also been shown to incorporate molecular events into direct physiological responses related to cancer. Several ARS family members are involved in promoting the formation of new microvasculature through angiogenesis, which could enhance the tumor growth capacity and facilitate metastasis.

1.3 Angiogenesis

1.3.1 Angiogenesis Background

Angiogenesis is the growth of new blood vessels from pre-existing vasculature, and is carried out in healthy and diseased tissue (Adair and Montani 2010). Because of its involvement in cancer, heart disease and other common diseases, angiogenesis has gained attention over the past few decades. Although the core mechanism of angiogenesis is well understood, there are other molecular players in different tissues and diseases that are involved in angiogenesis whose mechanisms of action remain unknown.

In a growing vertebrate embryo, mesodermal cells will ultimately differentiate into hematopoietic stem cells and angioblasts, which further differentiate into hematopoietic cells and endothelial cells respectively (Adair and Montani 2010). Endothelial cells arrange to form hollow tube structures that classify the vasculature. Therefore angioblast differentiation must be tightly regulated to ensure proper vasculogenesis in the developing embryo. Angiogenesis links two existing blood vessels together in poorly perfused tissue when the microenvironment becomes hypoxic (Adair and Montani 2010). When vascular endothelial cells are exposed to a high concentration of vascular endothelial growth factor (VEGF) under hypoxia they become tip-cells, which facilitate endothelial cell migration (Adair and Montani 2010). These tip-cells guide the new vasculature through the extracellular matrix, and ultimately lead to fusion with another blood vessel (Adair and Montani 2010). As aforementioned, this process is vital for tumor cell metastasis. VEGF also influences several ARSs' angiogenic activity.

VEGF is a pro-angiogenic autocrine signaling molecule in many cancers that aims to promote angiogenesis (Duffy, Bouchier-Hayes et al.). It is believed that VEGF translation may protect tumor cells from apoptosis as a result of this signaling. In breast carcinoma cells $\alpha 6\beta 4$ integrin signaling was found to upregulate VEGF translation, which led to an overall increase in cell survival (Chung, Bachelder et al. 2002). Specifically, $\alpha 6\beta 4$ integrin activates phosphoinositide-3 kinase (PI3-K) and protein kinase-B (Akt) pathways which stimulate the nutrient sensing mTOR. This causes the phosphorylation of 4E-binding protein (4E-BP), which allows eukaryotic initiation factor-4E (eIF4E) to dissociate from 4E-BP and stimulate VEGF translation specifically (Fig. 1) (Chung, Bachelder et al. 2002). The increase in VEGF expression protects breast carcinoma cells from apoptosis, and increases their chances of proliferation and angiogenesis.

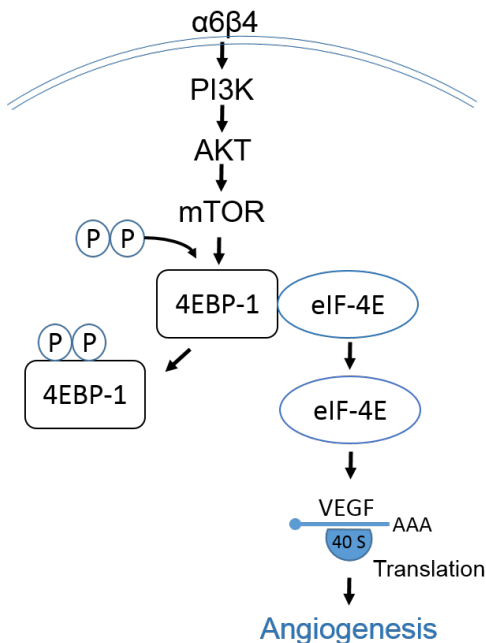


Figure 1: Mechanism of increased VEGF translation by $\alpha 6\beta 4$ integrin activation. Adapted from (Duffy, Bouchier-Hayes et al.).

1.3.2 Synthetase Angiogenic Activity

Several ARSs have been found to affect angiogenesis both intracellularly and extracellularly. YARS, WARS and TARS are secreted out of the cell, and stimulate signaling events extracellularly that affect angiogenesis while seryl-tRNA synthetase (SARS) and EPRS act intracellularly to change levels of VEGF transcription and translation, which alters the angiogenic state of the cell (Mirando, Francklyn et al. 2014). YARS is cleaved by polymorphonuclear leukocyte (PMN) elastase upon secretion from endothelial cells yielding N- and C-terminal fragments (Mirando, Francklyn et al. 2014). The N-terminus, or “mini-YARS”, is found to have catalytic activity and to stimulate angiogenesis through extracellular signal-regulated kinase (ERK) 1, ERK 2, Akt, Src and endothelial nitric oxide synthase (eNOS) signaling pathways (Mirando, Francklyn et al. 2014). These signaling pathways are pro-angiogenic, indicating likely involvement of VEGFR2 and integrin receptors (Munoz-Chapuli, Quesada et al. 2004). The C-terminus YARS fragment’s role is less characterized. WARS either undergoes a cleavage by PMN elastase once secreted from endothelial cells thus removing its WHEP domain, or WARS transcript can be alternatively spliced and translated yielding partial WARS that is then secreted from the cell (Mirando, Francklyn et al. 2014). The “mini-WARS” fragment then has an inhibitory effect on angiogenesis, which is a result of inhibition of phosphorylation of ERK, Akt and eNOS downstream targets and prevention of VEGF-mediated angiogenesis (Tzima, Reader et al. 2003). The secretion mechanism of both WARS and YARS remains unresolved.

SARS and EPRS alter VEGF expression intracellularly to inhibit angiogenesis. In endothelial cells SARS is transported to the nucleus by a nuclear localization signal, and

inhibits c-Myc-mediated *vegfa* transcription by altering the epigenetics of the *vegfa* gene (Mirando, Francklyn et al. 2014). This produces an angiostatic effect. The bi-functional EPRS is bound in the MSC under normal conditions. Upon treatment of endothelial cells with interferon- λ (IFN), EPRS is phosphorylated and dissociates from the MSC (Sampath, Mazumder et al. 2004). EPRS has been found to be a part of the IFN- λ -activated inhibitor of translation (GAIT) complex for binding ceruloplasmin mRNA (Sampath, Mazumder et al. 2004). Upon phosphorylation, EPRS will associate with this complex, and bind the 3' UTR of ceruloplasmin mRNA directly, which inhibits translation of the transcript (Sampath, Mazumder et al. 2004). This result was extended when it was found that the GAIT complex also binds the 3' UTR of VEGFA transcript thereby inhibiting VEGFA synthesis (Ray and Fox 2007). The WHEP domain of EPRS is responsible for this interaction. This shows that EPRS plays a role in inhibition of angiogenesis upon cytokine stimulation.

TARS exhibits extracellular, pro-angiogenic effects in endothelial cells. This property has predominantly been shown using the TARS inhibitor, borrelidin. Borrelidin is a compound produced in *S. rocheii*, which acts as an antibacterial, antiviral and antifungal agent. It is an 18-membered macrolide ring, and is a potent inhibitor of TARS as well as an inhibitor of angiogenesis and metastasis in various rat models (Mirando, Fang et al. 2015). Due to its strong inhibition of TARS, borrelidin is highly cytotoxic to cells, which is a result of the amino acid starvation response (Mirando, Fang et al. 2015). BC194 is a borrelidin analog that is less toxic to cells, but inhibits TARS just as strongly as borrelidin due to maintenance of key substrate binding residues in the active site (Mirando, Fang et al. 2015). Endothelial cells show decreased tube formation in tube

assays, a model for angiogenesis, and decreased cell migration upon treatment with BC914 (Williams, Mirando et al. 2013, Mirando, Fang et al. 2015). The anti-angiogenic property of BC194 has been confirmed *in vivo* using zebrafish as a model organism (Mirando, Fang et al. 2015). In addition, chorioallantoic membrane (CAM) assay on chicken embryos reveal that when TARS is added exogenously to embryos the vasculature expands, and when TARS is added exogenously to endothelial cells tube formation increases (Williams, Mirando et al. 2013). These findings confirm that TARS is pro-angiogenic. Similar to WARS and YARS, the secretion mechanism remains unknown for TARS. However, upon treatment with VEGF or TNF- α , endothelial cells have an increase in TARS in the cell culture media (Williams, Mirando et al. 2013). This further suggests that TARS is secreted for the purpose of promoting angiogenesis.

1.3.3 Possible Mechanism of Synthetase Secretion

One possible mechanism that synthetases are getting secreted out of cells is by exosomal release. Exosomes are small vesicular particles between 40-100 nm in diameter that are vital for cell signaling as they have been found to contain specific RNA and protein cargo. There is no definite consensus on how exosomes are secreted out of cells, however the predominant theory will be discussed here. Early endosomes pinch towards the cytosol from the plasma membrane of the secreting cell (Bobrie, Colombo et al. 2011). Early endosome maturation to a multivesicular body (MVB) is characterized by further pinching of the membrane away from the cytosol, and towards the extracellular space. These smaller vesicles in the MVB are often exosomes. The MVB then fuses with

the plasma membrane releasing its contents, and the exosomes are secreted from the cell (Fig. 2) (Bobrie, Colombo et al. 2011).

Various families of proteins known to facilitate vesicular trafficking and docking are thought to enable this process. Exosomes can be tracked experimentally by looking at proteins bound in exosomal membranes, including CD63 and MHC class II proteins (Bobrie, Colombo et al. 2011). In this study, we observed changes in CD63 protein levels to draw conclusions about exosome production in ovarian cancer cells.

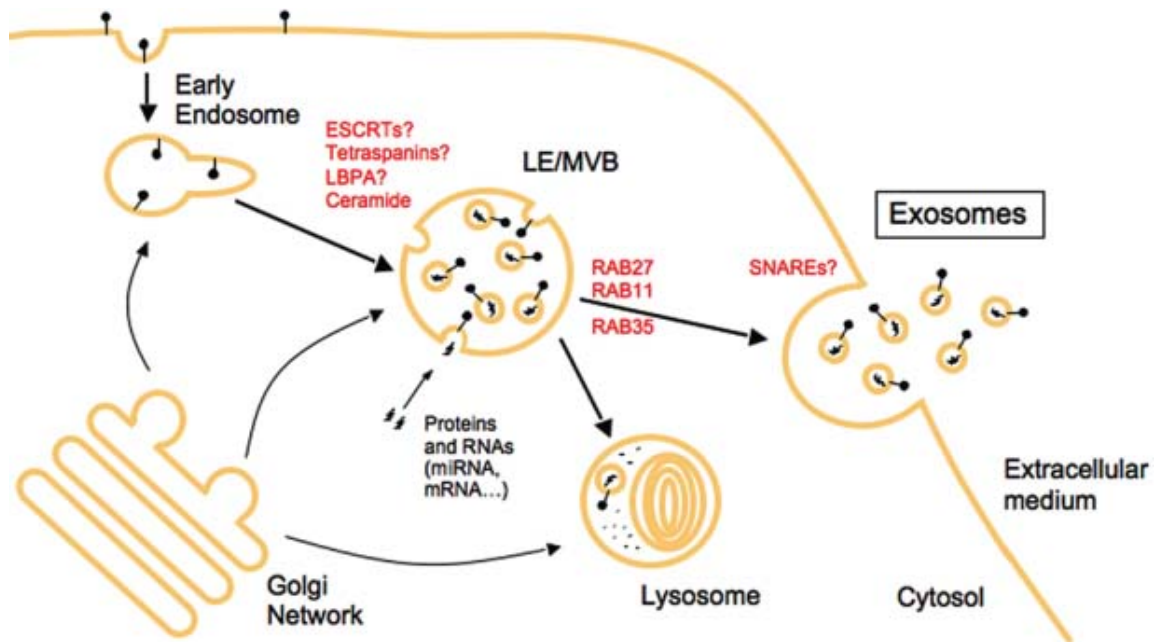


Fig. 2: Proposed mechanism of exosome formation and subsequent release. Used with permission from (Bobrie, Colombo et al. 2011).

It has been observed that cytoplasmic synthetase mRNA from several family members is found in exosomes in Jurkat cells (Wang, Xu et al. 2013). This raises the question of what role these mRNA will ultimately play translationally, and begins to outline possible mechanisms for ARS secretion. In addition, many members of the ARS

family have been identified in exosomes of cancer cells. A large scale proteomic analysis found that several cytoplasmic and mitochondrial synthetase proteins can be found in both OVCAR-3- and IGROV1-, two ovarian cancer cell lines, derived exosomes, including TARS (Liang, Peng et al. 2013). With knowledge that extracellular TARS is pro-angiogenic in endothelial cells and that TARS is found in ovarian cancer cell-derived exosomes, we aimed to test whether TARS was secreted from ovarian cancer cells via exosomal release in order to further the mechanism by which TARS promotes angiogenesis.

1.4 Endoplasmic Reticulum Stress Response

1.4.1 Endoplasmic Reticulum Stress and the Unfolded Protein Response

When cells are diseased they experience some level of stress, which is characterized by stimulation of the immune response, changes in intracellular molecular status or an alternate response. One specific type of stress response is endoplasmic reticulum (ER) stress. The ER is responsible for facilitating proper protein folding, and when unfolded protein accumulates the unfolded protein response (UPR) will be elicited. The UPR is a complex web of molecular cascades that trigger either a survival response or an apoptotic response following ER stress.

Three receptors are bound in the ER membrane that regulate the UPR, inositol-requiring protein-1 α (IRE1 α), PRKR –like ER kinase (PERK) and activating transcription factor 6 (ATF6) (Oslowski and Urano 2011). IRE1 α and PERK have similar ER-luminal domains and cytosolic kinase domains while ATF6 has a cytosolic cAMP

response element binding protein (CREB)-ATF basic leucine zipper domain (Wang and Kaufman 2016). All receptors constitutively bind immunoglobulin protein (BiP) on the ER-luminal side. Upon misfolded protein accumulation, BiP binds the misfolded protein and leaves the receptors nude. Nude receptors are believed to activate the UPR (Wang and Kaufman 2016). Activation of these three signaling cascades initially triggers three transcription factors that promote transcription of genes involved in protein folding and quality control, ER biogenesis, autophagy and other processes that aid in proper protein folding (Hetz 2012). IRE1 α dimerizes and autophosphorylates upon activation, and facilitates splicing of X-box-binding protein-1 (XBP1) mRNA, which allows XBP1s to act as a transcription factor for genes promoting cell survival (Wang and Kaufman 2016). PERK and ATF6 pathways have also been shown to play a role in induction of XBP1 and its splicing, highlighting interplay often found in the UPR (Yoshida, Matsui et al. 2001, Tsuru, Imai et al. 2016). PERK dimerizes and autophosphorylates upon activation, which leads to phosphorylation of Ser51 on eukaryotic initiation factor-2 α (eIF2 α) thereby inhibiting global protein translation (Wang and Kaufman 2016). Phosphorylation of eIF2 α also induces translation of ATF4, which acts as a transcription factor for survival-promoting genes (Hetz 2012). ATF6 activation leads to ATF6 α transit to the Golgi apparatus where it is cleaved by the enzymes S1P and S2P, and this cleavage product acts as a transcription factor at target genes (Wang and Kaufman 2016). These pathways promote proper protein folding and cell survival, which classifies the adaptive response (Fig. 3).

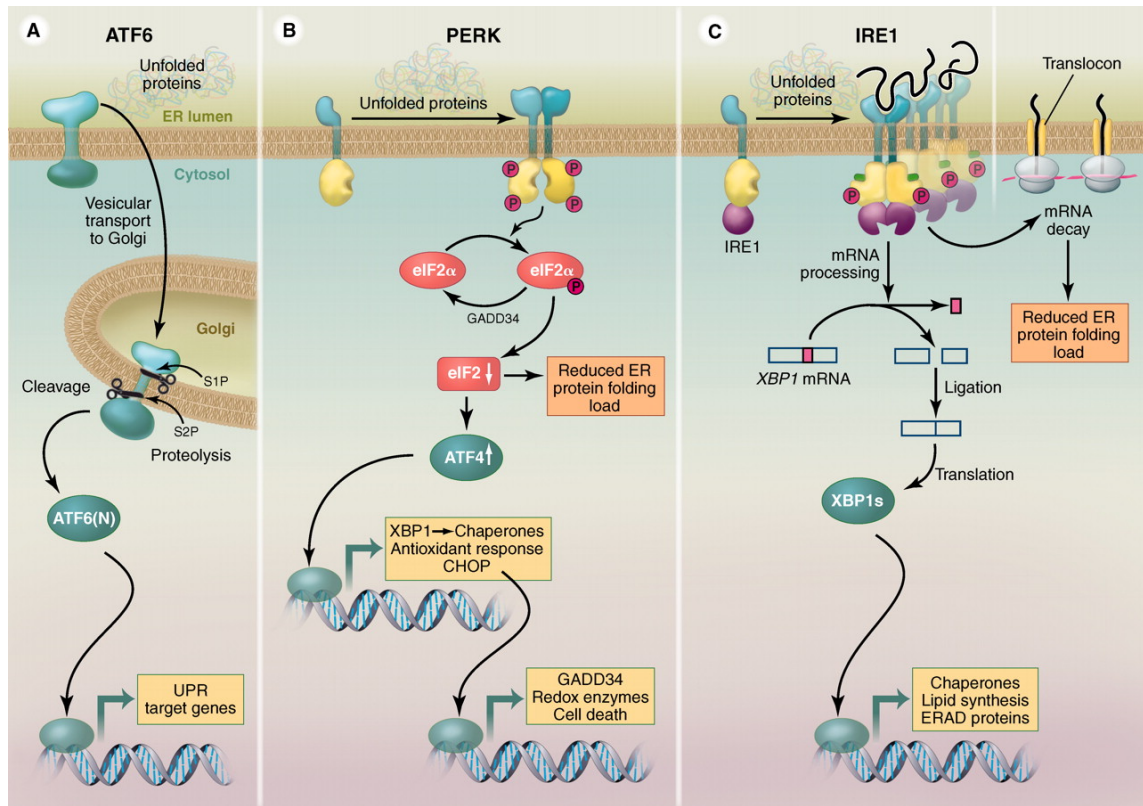


Fig. 3: Diagram of UPR signaling pathways. Used with permission from (Walter and Ron 2011).

The maladaptive UPR occurs as time of the ER stress increases, which subsequently increases the intensity of the stress. The maladaptive response results in apoptosis. Following prolonged exposure to tunicamycin or thapsigargin, two known ER stressors, fibroblasts exhibit decreased XBP1 mRNA splicing, increased full-length ATF6 coupled with decreased active ATF6, and increased p-eIF2 α and ATF4 (Lin, Li et al. 2007). Levels of CHOP, a pro-apoptotic protein downstream of PERK, are also increased, suggesting an alternative function for ATF4 (Lin, Li et al. 2007). Additionally, in an ER stress model in *Drosophila*, PERK was found to independently trigger apoptosis (Demay, Perochon et al. 2014). Taken together, these data indicate that under prolonged

ER stress IRE1 α and ATF6 pathways are diminished and sustained PERK activity leads to apoptosis. This outcome is likely a result of inability of the cell to facilitate proper protein folding, and so to avoid mutation or dysfunction it undergoes apoptosis.

1.4.2 General Control Nonderepressible 2

The ARS family's vital role in translation renders these enzymes likely players in the UPR. ARSs can act as nutrient detectors due to their interactions with amino acids. When specific amino acids are absent, ARSs will not be able to carry out aminoacylation reactions leading to loss of function. This amino acid deprivation response can be detected by the protein complex general control nonderepressible 2 (GCN2). Similar to PERK, GCN2 is activated by amino acid deprivation, and catalyzes phosphorylation of eIF2 α (Hamanaka, Bennett et al. 2005). This regulation occurs independent of ER stress and PERK induction, however both PERK and GCN2 aim to regulate protein synthesis through eIF2 α phosphorylation and cell cycle control (Hamanaka, Bennett et al. 2005). Interestingly, in yeast GCN2 and HARS have a region of homology between them, which in HARS is located near its catalytic core (Wek, Zhu et al. 1995). It was found that phosphorylation of eIF2 α was observed under amino acid starvation conditions, including histidine starvation, and that HARS interacts directly with GCN2, which can impair GCN2's ability to phosphorylate eIF2 α upon HARS mutation (Wek, Zhu et al. 1995). Additionally, uncharged tRNA molecules regulate GCN2 activity more so than the actual amino acid starvation response (Wek, Zhu et al. 1995). Uncharged tRNA was confirmed as the primary regulator of GCN2 in CHO-K1 cells with mutant LARS

(Harding, Novoa et al. 2000). This finding suggests ARS involvement in a key regulatory step that overlaps with the UPR.

1.4.3 Synthetase Involvement in ER Stress

TARS inhibition by borrelidin causes amino acid starvation, which leads to cytotoxicity, and phosphorylation of eIF2 α (Mirando, Fang et al. 2015). This indicates that borrelidin is either triggering GCN2 activation by increasing the pool of uncharged tRNA, or is affecting the rate of translation and inducing the UPR. In addition, borrelidin induces caspase-3 cleavage suggesting that borrelidin may be causing apoptosis via the PERK UPR response pathway, however this remains to be confirmed (Mirando, Fang et al. 2015). In oral cancer cells, borrelidin was found to trigger CHOP-mediated apoptosis indicating TARS involvement in the UPR (Sidhu, Miller et al. 2015). In this study however, the concentration of borrelidin used and the time cells were treated with borrelidin were both much higher than other reported literature values. This evidence validates TARS as a potential target for UPR intervention.

It has also been reported that KARS is highly dependent on the UPR to promote hypoxia resistance in *C. elegans* (Anderson, Mao et al. 2009). By transfecting with a decrease in KARS function mutant, *C. elegans* shows an increase in hypoxia resistance, which is inversely proportional to rate of translation (Anderson, Mao et al. 2009). Additionally, hypoxia triggers the UPR, and using a dual decrease in functional KARS/*ire1* gene knockout *C. elegans*, this hypoxia resistance was lost (Anderson, Mao et al. 2009). This indicates that KARS not only regulates translation rate in *C. elegans*,

but can also regulate hypoxia resistance given UPR induction occurs following hypoxia onset.

1.4.4 Monensin

Given the current connection between ARSs and the UPR, the question of what exact mechanisms comprise this connection arises. To tease out which “flavor” of ER stress different synthetases are involved in, different ER stressors must be examined. Monensin is a polyether, monovalent ionophore that acts on the Na^+/H^+ transmembrane pump, which subsequently collapses the Na^+/H^+ gradient maintained across the plasma membrane (Mollenhauer, Morre et al. 1990). This leads to an increase in intracellular Na^+ , and a subsequent increase in intracellular Ca^{+2} (Meral, Hsu et al. 2002). Monensin has been linked to stimulation of exosomal release as a result of its effects on intracellular Ca^{+2} concentrations (Savina, Furlan et al. 2003, Guo, Bellingham et al. 2016). In addition to its role in exosomal release, monensin has been linked to ER stress. One study found monensin was able to sensitize glioma cells to tumor necrosis factor-related apoptosis-induced ligand (TRAIL)-mediated apoptosis through ER stress. Monensin led to an increase in ATF4, CHOP and p-eIF2 α expression in glioma cells and decreased overall cell viability (Yoon, Kang et al. 2013). Monensin has been used to monitor ER stress in other studies as well (Badr, Hewett et al. 2007). Given the relatively undeveloped nature of the mechanism by which monensin induces ER stress, experimental data of monensin effects on synthetases would be invaluable. In the present study, we aim to further characterize the effects that monensin has on TARS levels intracellularly and extracellularly.

1.5 Experimental Model

We hypothesized that the mechanism for TARS secretion from human ovarian cancer cells was by exosomal packaging and subsequent release. We also hypothesized that intracellular TARS expression was effected by ER stress, and that this would affect the pro-angiogenic function of TARS. We measured TARS levels by Western blotting, reverse transcriptase-quantitative polymerase chain reaction (RT-qPCR), immunofluorescence (IMF) microscopy and exosome precipitation from media and subsequent Western blotting. We used monensin as a dual exosomal release stimulator and ER stressor. Upon stimulation with monensin, CaOV-3 cells had higher levels of TARS protein in the cell media compared to control, untreated cells. However when these media samples had exosomes precipitated out there was no difference in the CD63 marker protein across samples. Monensin treatment caused TARS protein and transcript levels to increase in CaOV-3 cells, and also induced markers of ER stress at the transcript and protein level. Also noteworthy is we were able to show a significant increase in VEGF transcript levels in CaOV-3 cells in response to monensin treatment. These data indicate that CaOV-3 cells increase TARS expression and secretion in response to ER stress.

CHAPTER 2: EXPERIMENTAL PROCEDURES AND MATERIALS

Cell Culture

CaOV-3 human ovarian cancer cells were purchased from American tissue culture (ATCC), and cultured in Dulbecco's Modified Eagle's Medium (DMEM) high glucose (4500 mg glucose/L) (GE Healthcare or Sigma). Media was supplemented with 1% L-glutamine, 1% penicillin/streptomycin and 10% fetal bovine serum (FBS). Cells were maintained between passages 2 and 16, and were split once they reached 70-100% confluence. Cells were grown in 21% oxygen, 5% CO₂ and 37°C in a humidified incubator. Cell treatments were done overnight, 16-20 h, unless otherwise specified.

Reagents

Cell Culture treatments

- Monensin (Sigma)
- VEGF (R&D Systems)
- Dimethyl sulfoxide (DMSO) (Fischer Bioreagents)
- Borrelidin (Biotica Technology, LTD)

Primary Antibodies for Western Blotting

- Rabbit anti-TARS (GeneTex #GTX116359) at 1:1000
- Mouse anti-CD63 (Novus #NB100-77913) at 1:1000
- Rabbit anti- β -tubulin (Cell Signaling #2128) at 1:1000
- Rabbit anti-LARS (Protein Tech #21146-1-AP) at 1:1000

- Rabbit anti-AARS (GeneTex #GTX112477) at 1:1000
- Rabbit anti-p-eIF2 α (Cell Signaling #9721) at 1:1000
- Rabbit anti-eIF4E2 (GeneTex #GTX82524) at 1:250
- Rabbit anti-RBM4 (Protein Tech #11614-1-AP) at 1:1000
- Rabbit anti-Hif-2 α (Novus #NB100-122) at 1:1000

*All dilutions made in 3% BSA/TBST. Solutions also contain 0.1% sodium azide

Primary Antibodies for Immunofluorescence

- Mouse anti-TARS (Abnova #H00006897-M01) at 1:200
- Rabbit anti-TARS (GeneTex #GTX116359) at 1:200
- Mouse anti-CD63 (Novus #NB100-77913) at 1:50
- Rabbit anti-vimentin (Cell Signaling #5741) at 1:200

Western blotting

Cells were seeded on 10 cm plates and grown to 70-100% confluence prior to treatment. Treatments were done in serum-free media unless otherwise specified.

Following treatment, media was collected and cell monolayers were washed in phosphate buffered saline (PBS) (Thermo Scientific) twice, and then lysed in modified RIPA buffer (150 mM NaCl, 50 mM Tris pH 8.0, 5 mM EDTA, 0.5% deoxycholate, 1% NP-40, 10% glycerol; Protease inhibitors: 2 mM Na pyrophosphate (Sigma), 1 mM phenylmethane sulfonyl fluoride (PMSF) in ethanol (Sigma), 111.17 KIU/mL aprotinin (Fischer)). Media

was concentrated 10-fold using Amicon®-Ultra 4-Centrifugal Devices 30,000 MWCO, and lysate was homogenized using a 25-gauge syringe. To correct for loading, a Bradford Assay was performed on each sample for each experiment (Bradford 1976). Samples were prepared in 4X Laemmli sample buffer (0.2 M Tris pH 6.8, 4% Sodium dodecyl sulfate (SDS), 4 mg/mL bromophenol blue, 4% β -mercaptoethanol, 40% glycerol, 4 μ M pyronin Y), and resolved on Mini-PROTEAN TGX Stain-Free Precast Gels (Bio-Rad) for 15-20 min at 300V. Gels were transferred to PVDF membrane for 75 min at 4°C. Washes were done in Tris-buffered saline and Tween-20 (TBST). Blots were blocked in 3% milk in BSA/TBST for 30 min at room temperature with rocking and then incubated in primary antibodies overnight at 4°C. Secondary antibodies used were either horseradish peroxidase (HRP)-goat-anti-rabbit IgG (Santa Cruz) at 1:5000 or HRP-goat-anti-mouse IgG (Santa Cruz) at 1:5000 in 3% BSA/TBST. Antibody-bound proteins were detected by chemilluminescence. Blots were either developed on X-ray film or scanned on the VersaDoc 4000 MP (BioRad) using Pierce ECL Western Blotting Substrate or Super Signal West Femto Maximum Sensitivity Substrate (Thermo Scientific) as needed. Bands were analyzed using Quantity One 1-D Analysis Software for densitometry (BioRad). β -tubulin was used as a loading control.

Blots shown with multiple proteins are the same membrane reprobed with different primary antibodies. Following chemilluminescent detection, blots were washed in stripping buffer (1.5% glycine, 0.1% SDS, 1% Tween-20 at pH 2.2). Blots were then reblocked and reprobed with respective primary antibodies.

Exosome Precipitation

Cells were seeded on 10 cm plates and grown to 70-90% confluence prior to treatment. Cells were treated using 10% FBS, exosome-depleted media (System BioSciences). Following treatment, media was collected and exosome isolation was performed according to manufacturer protocol. Cell lysates were not collected. Briefly, ExoQuick-TC™ Tissue Culture Media Exosome Precipitation Solution (System Biosciences) was added to media samples at 1 ml ExoQuick: 5 mL cell culture media. Samples were mildly agitated and incubated for 16 h at 4°C. Following incubation, samples were spun and the pellet, which contained exosomes, was resuspended in PBS. These samples were frozen at -80°C, which lysed exosomes, and samples were then resolved by Western blot. 10% FBS, exosomes-depleted media that was not exposed to cells was resolved by Western blot as a negative control.

Immunofluorescence Microscopy

Cells were seeded on glass coverslips in a six-well plate, and grown to 90% confluence prior to treatment. Following treatment, media was removed from the wells. Cells were fixed in 10% formalin (Sigma-Aldrich) for 15 min at room temperature, and then were treated with 100% methanol (Sigma-Aldrich) for 2 min at room temperature to promote membrane permeabilization. Each slide was then incubated in a primary antibody solution for 16 h at 4°C in a humidity box. Primary antibody solutions consisted of Novus mouse anti-TARS and anti-vimentin in one solution and GTX rabbit anti-TARS and anti-CD63 in another, diluted in 3% BSA/0.2% Triton X-100 (TX-100)/PBS. Following incubation in primary antibody, wells were incubated in a secondary antibody

solution of Alexa 488 donkey anti-mouse IgG (Invitrogen) at 1:500, Alexa 594 donkey anti-rabbit IgG (Invitrogen) at 1:500 and 10µg/mL of 4'-6-Diamidino-2-phenylindole dihydrochloride (DAPI) (Roche Diagnostics) in 3% BSA/0.2% TX-100/ PBS for 1 h at 37°C in the dark. Coverslips were then mounted on *Superfrost*® Microscope Slides (Fisherbrand) using Aqua Poly/Mount (Polysciences Inc.) and stored flat in the dark at 4°C prior to imaging. Slides were imaged within 1-5 days using the Nikon TE 200 inverted epifluorescence microscope from Dr. Alan Howe's lab.

Reverse Transcriptase-quantitative Polymerase Chain Reaction (RT-qPCR)

Cells were seeded in a six-well plate, and grown to 90-100% confluence prior to treatment. Following treatment, total RNA was extracted from cells using the RNeasy® Plus Mini Kit (Qiagen) according to manufacturer's instructions. Total RNA concentration was determined using NanoDrop ND-1000 (Thermo Fischer) for each sample. An equal mass of RNA from each sample for each trial was used to synthesize first strand cDNA using High Capacity cDNA Reverse Transcription Kit (Applied Biosystems), which includes MultiScribe Reverse Transcriptase (Applied Biosystems). RT-qPCR was performed using an ABI Prism 7900HT Sequence Detection System (Applied Biosystems) and TaqMan® Assay Primer pairs (Applied Biosystems) for *tars*, *lars*, *aars*, *vegfa* and *dnajb9*.

During the PCR reaction, Taq polymerase will knock the fluorophore off the target gene, which emits fluorescence and is measured by the PCR detection system. The emitted fluorescence is directly proportional to the gene expression, as measured by threshold cycle (CT) values. Relative mRNA expression was determined using a

comparative CT ($\Delta\Delta\text{CT}$) method, and target genes were normalized to the *hpri* gene as the housekeeping gene. All RT-qPCR work was performed in the University of Vermont Cancer Center DNA Analysis Facility and was supported in part by grant P30CA22435 from the NCI.

Immunoprecipitation

Cells were seeded on 10 cm. plates, and grown to 60-80% confluence prior to treatment. Following hypoxic treatments, cells were lysed in 1X cell lysis buffer (CLB) (20 mM Tris pH 7.5, 150 mM NaCl, 1 mM EDTA, 1 mM EGTA, 1% TX-100; Protease inhibitors: 2.5 mM Na pyrophosphate, 1 mM Na orthovanadate, 1 $\mu\text{g}/\text{mL}$ leupeptin, 1 mM PMSF in EtOH, 1 $\mu\text{g}/\text{mL}$ aprotinin), and lysates were homogenized using a 25-gauge syringe. TARS protein was pulled down from solutions using Dynabeads® M-280 Sheep anti-Mouse IgG (Thermo Fischer) bound to Novus mouse anti-TARS antibody. Protein bound to the beads was eluted off in Laemmli 4XSB and high heat. Total lysate, supernatant following the pull down and protein eluted from the beads was resolved by Western blot for each sample. The “no antibody control” refers to a sample that was exposed to Dynabeads that were not bound to Novus mouse anti-TARS antibody. This sample should not have any TARS or associated proteins in the pull down.

Separation of Nuclear Cell Lysate from Cytoplasmic Cell Lysate

Cells were seeded on 10 cm plates and grown to 90% confluence. Following treatments, media was removed, and cells were lysed in hypotonic lysis buffer (1 M Tris pH 8.0, 1 M MgCl_2 , 2 M KCl; Protease inhibitors: 100 mM PMSF in EtOH, 2 mg/mL

Aprotinin, 2 mM Na Pyrophosphate). Total cell lysate was spun at 1000 x g, 5 min, which pellets the nuclear fragment. Cytosolic supernatant was removed, and the nuclear pellet was washed in hypotonic lysis buffer. The pellet was resuspended in hypotonic lysis buffer. Samples were resolved by Western blot.

CHAPTER 3: EXTRACELLULAR TARS PROTEIN LEVELS INCREASE IN CAO-3 CELLS IN RESPONSE TO MONENSIN TREATMENT WHILE CD63 PROTEIN IS UNAFFECTED

3.1 Introduction

SKOV-3 cells, a human ovarian cancer cell line, overexpress TARS and show colocalization of TARS with pro-angiogenic markers (Wellman, Eckenstein et al. 2014). This renders human ovarian cancer cells as a valid *in vitro* model to study TARS and its effects on angiogenesis. TARS also promotes angiogenesis and cell migration extracellularly in endothelial cells (Williams, Mirando et al. 2013). We hypothesize that TARS is secreted from cells via exosomal release, as there is evidence for synthetase protein and mRNA packaging in exosomes (Liang, Peng et al. 2013, Wang, Xu et al. 2013). To test for this we used an exosome stimulator, monensin, as a means to increase TARS secretion from CaOV-3 cells.

3.2 Results

To first test the hypothesis that monensin stimulates TARS secretion, we performed Western blots on concentrated cell media from CaOV-3 cells treated with monensin compared to control. Upon treatment with 10 μ M monensin, TARS protein levels increased in the cell media compared to a DMSO control (Fig. 4). The stock solution of monensin was dissolved in DMSO, and so DMSO was used as the control treatment to ensure all cell plates received equal volumes of DMSO. DMSO increases the permeability of lipid membranes, and so it is important to maintain experimental groups

in equal volumes of DMSO (Notman, Noro et al. 2006). This initial finding confirms that monensin is causing TARS protein levels to increase in the cell media.

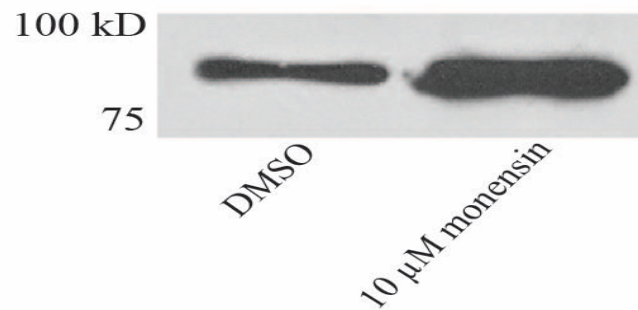


Figure 4: TARS is secreted out of CaOV-3 cells in response to monensin treatment. Western blot of concentrated cell media using an antibody against TARS. Cells were treated in serum-free media with respective reagents for 16 h before media was collected. Media samples were concentrated 12-fold. Blot was not quantified, but this result was duplicated.

With knowledge that TARS protein levels increased in CaOV-3 cell media following treatment with monensin, we next wanted to determine if the extracellular TARS we were detecting was packaged in exosomes. CaOV-3 cells were treated in 10% FBS, exosome-depleted media. Cell media was incubated with ExoQuick-TC™ solution, which precipitates exosomes out of solution. The exosome precipitant was pelleted, and resuspended in PBS. Samples were then resolved by Western blot and anti-TARS and anti-CD63 antibodies were used to detect protein (Fig. 5A). CD63 is an exosomal marker protein that is expressed on ovarian cancer-derived exosomes as well as breast cancer-derived exosomes (Gercel-Taylor, Atay et al. 2012, King, Michael et al. 2012). We found that monensin and VEGF treatments both led to an increase in extracellular TARS

protein following exosome precipitation compared to the DMSO control (Fig. 5C), however this increase does not correspond to a change in CD63 protein levels (Figs. 5B). This confirms our initial result regarding increased levels of extracellular TARS protein in response to monensin treatment, and shows that extracellular TARS protein levels also increase in response to VEGF in CaOV-3 cells, similar to prior results in endothelial cells (Williams, Mirando et al. 2013). However, we fail to show extracellular TARS is secreted in exosomes. These trends did not match statistical significance.

IMF microscopy staining for CD63 further confirmed that neither monensin nor VEGF treatment of CaOV-3 cells causes an increase in CD63 protein levels. These images represent intracellular TARS and CD63. Monensin and VEGF both failed to cause an increase in intracellular CD63 (Fig. 6). The CD63 staining pattern is “spotted” and localized throughout the cytoplasm, which aligns with expected MVB distribution (Pols and Klumperman 2009). It can be assumed that the anti-CD63 antibody is marking exosomes that are either destined for secretion, or are being endocytosed from the extracellular space. In addition, intracellular TARS protein increases in CaOV-3 cells when treated with monensin or VEGF (Fig. 6). These results further our claim that monensin and VEGF treatments increase TARS protein levels, however this increase is not coupled with an increase in CD63 protein. The mechanism of TARS secretion therefore remains unresolved.

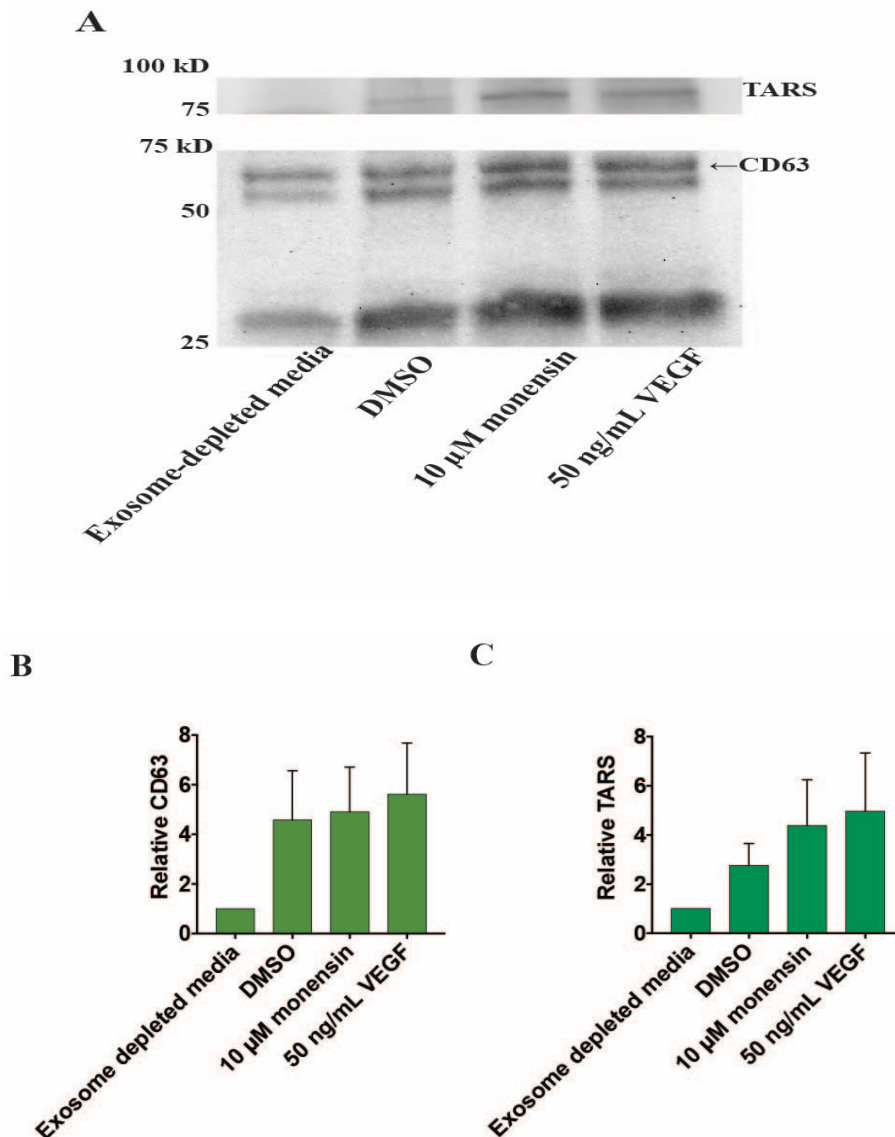


Figure 5: TARS protein secretion increases with monensin and VEGF cell treatments while CD63 is unaffected. (A) Western blot of exosomes precipitated out of cell media using antibodies against TARS and CD63. CaOV-3 cells were treated in exosome-depleted media and respective reagents. Cell media was collected and exosomes were precipitated out of solution using ExoQuick-TC™. A sample of exosome-depleted media was run as a negative control. The banding pattern on the lower blot was only observed in this trial, while the band indicated as CD63 could be replicated. CD63 is between 26-60 kD depending on its glycosylation state, which is why all three bands are shown. (B,C) Quantification of CD63 (B) and TARS (C) protein levels normalized to the negative control; mean \pm SEM, n=3, p>0.05 comparing experimental groups and negative control and comparing 10 μ M monensin and 50 ng/ml VEGF treatments with DMSO control (Kruskal-Wallis, Dunn's multiple comparisons test).

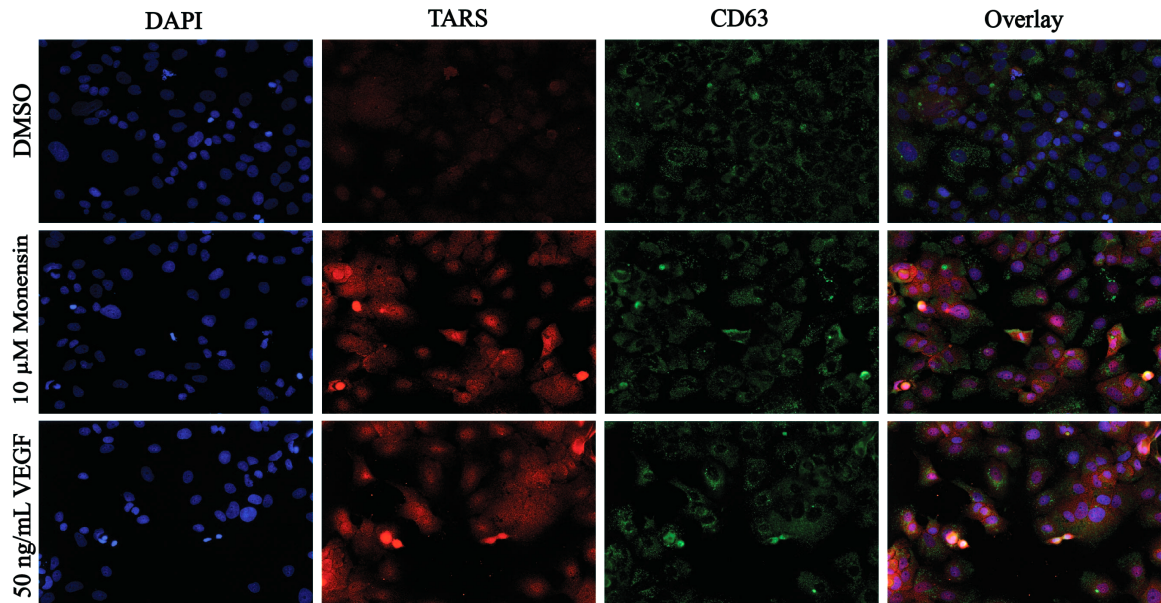


Fig. 6: Monensin and VEGF treatments of CaOV-3 cells do not affect intracellular CD63 protein levels. CaOV-3 cells were grown on glass cover slips and treated in 10% FBS. Cells were treated with DMSO, 10 μ M monensin or 50 ng/mL VEGF for 18h. Cells were fixed with 10% formalin and stained with DAPI, rabbit anti-TARS and mouse anti-CD63 antibodies. DAPI, TexasRed and FITC channels were used to acquire images.

We conclude that both monensin and VEGF increase the extracellular concentration of TARS protein in CaOV-3 cells, however this increase is not confirmed to be a result of exosomal release. Although there is an increase in CD63 protein compared to the negative control (Fig. 5B), there is no increase when comparing monensin- or VEGF-treated cells to DMSO-treated cells. This confirms the presence of exosomes in experimental samples, but fails to confirm our hypothesis. Therefore, TARS protein levels increase extracellularly in response to either monensin or VEGF, but the mechanism of secretion remains unresolved.

CHAPTER 4: INTRACELLULAR TARS LEVELS IN CAO-3 CELLS ARE AFFECTED BY MONENSIN TREATMENT

4.1 Introduction

Many ARS genes are downstream targets of ATF4 and CHOP transcription factors in the UPR (Han, Back et al. 2013). This exemplifies how the maladaptive ER stress response induces transcriptional regulation of protein synthesis. TARS inhibition by borrelidin triggers the PERK maladaptive UPR through phosphorylation of eIF2 α , and cleavage of caspase-3 (Mirando, Francklyn et al. 2014). This shows further induction of the UPR by disruption of protein synthesis. Here we wanted to investigate how ER stress that is separate from TARS inhibition affects TARS protein and transcript levels in ovarian cancer cells.

4.2 Results

First we observed how intracellular TARS protein levels were affected in CaOV-3 cells following monensin treatment. CaOV-3 cells were treated with either DMSO or 10 μ M monensin in serum-free media, and total cell lysates were resolved by Western blot. We probed these blots with anti-TARS, anti-LARS and anti-AARS antibodies (Fig. 7A). LARS and AARS were used to test whether results we observed with TARS were TARS-specific, or whether these results could be extended to other synthetase proteins.

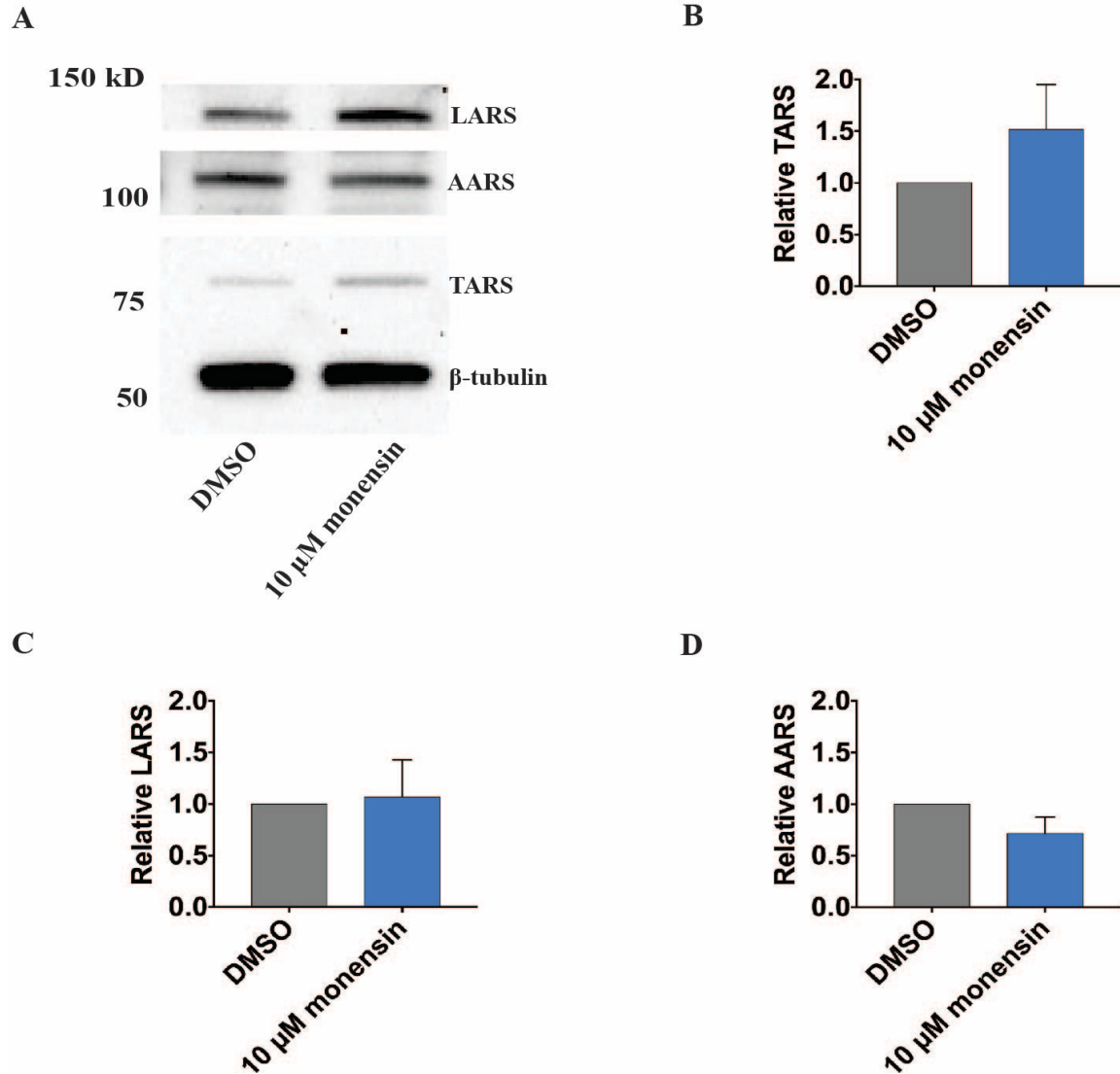


Fig. 7: TARS protein increases intracellularly in response to monensin by Western blot. (A) Western blot of total cell lysates from CaOV-3 cells treated with respective reagents using antibodies against TARS, LARS and AARS. (B-D) Quantified protein values for TARS (B), LARS (C) and AARS (D) relative to a β -tubulin loading control. Samples were normalized to DMSO; mean \pm SEM, n=4, p>0.05 comparing 10 μ M monensin and DMSO (Wilcoxon signed-rank test).

We observed that in CaOV-3 cells, monensin induced an increase in expression of intracellular TARS protein (Fig. 7B), although the consistent trend did not match statistical significance. LARS protein levels did not change in response to monensin (Fig.

7C), and AARS protein levels decreased (Fig. 7D). More experimental trials would be necessary to confirm this result, and gain statistical significance. The lack of significance may also owe to the inconsistent nature of Western blotting.

This result shows that TARS protein levels increase in response to an ER stressor that does not inhibit synthetase activity. The increase in TARS and not LARS or AARS indicates TARS protein is playing a specific role in response to ER stress separate from global synthetase expression. Interestingly, monensin caused AARS protein levels to decrease.

Intracellular TARS increasing in response to monensin was also observed by IMF microscopy. CaOV-3 cells treated in both 0.1% FBS and 10% FBS (low and high serum, respectively) media exhibit an increase in TARS staining with monensin treatment (Figs. 8A-B). This increase is not seen following VEGF treatment. Vimentin is a common intermediate filament expressed in mesenchymal cells, which has recently been found to be overly expressed in tumor cells and to be a good marker of epithelial-to-mesenchymal transition (Eriksson, Dechat et al. 2009, Satelli and Li 2011). We did not expect vimentin expression to change in response to either monensin or VEGF, and so it was used here to confirm cytoplasmic integrity. There is a clear increase in TARS staining with monensin treatment, and this increase is most apparent in the low serum-treated cells (Fig. 8A). Low serum and monensin both highly stress the cells, which is correlated with an increase in TARS protein expression. TARS protein is localized in the cytoplasm with punctate structures distributed throughout.

We also found that monensin treatment decreased DAPI staining in both low and high serum-treated cells compared to DMSO controls, although the decrease was more

pronounced in low serum (Figs. 8A-B). DAPI stains cell nuclei, which confirms cell integrity upon formalin fixing. This indicates that cell death occurred as a result of monensin treatment, as cells were grown to equal confluence prior to treatments.

However, even with the decrease in DAPI staining, monensin still caused an increase in TARS staining. Taken together with the Western blots of concentrated CaOV-3 cell media (Fig. 4) and CaOV-3 total cell lysates (Fig. 7A), these data indicate that the observed increases in TARS protein in response to monensin treatment are a result of increased TARS expression, and not uncontrolled detection due to cell death.

Intracellular TARS protein localizes in the cytoplasm of CaOV-3 cells regardless of treatment (Fig. 9). This aligns with the literature, which reports TARS localization in both the cytoplasm and the mitochondria of the bacterium *T. brucei* (Kalidas, Cestari et al. 2014). TARS localization in the cytoplasm was observed by both IMF microscopy (Fig. 8) and by Western blot (Fig. 9). We therefore conclude that ER stress stimulated by monensin does not affect TARS localization.

To assess whether TARS induction by monensin was at the level of gene transcription, its effect on TARS and other ARS mRNA transcript levels was investigated. Transcript levels in CaOV-3 cells were quantified using RT-qPCR following respective treatments. Probes for AARS and LARS were used to test whether or not the TARS response was TARS-specific or if it was a general synthetase response.

Following monensin treatment, TARS transcript levels increased 2-fold (Fig. 10B). To confirm ER stress at the transcript level, DNAJB9 mRNA was quantified.

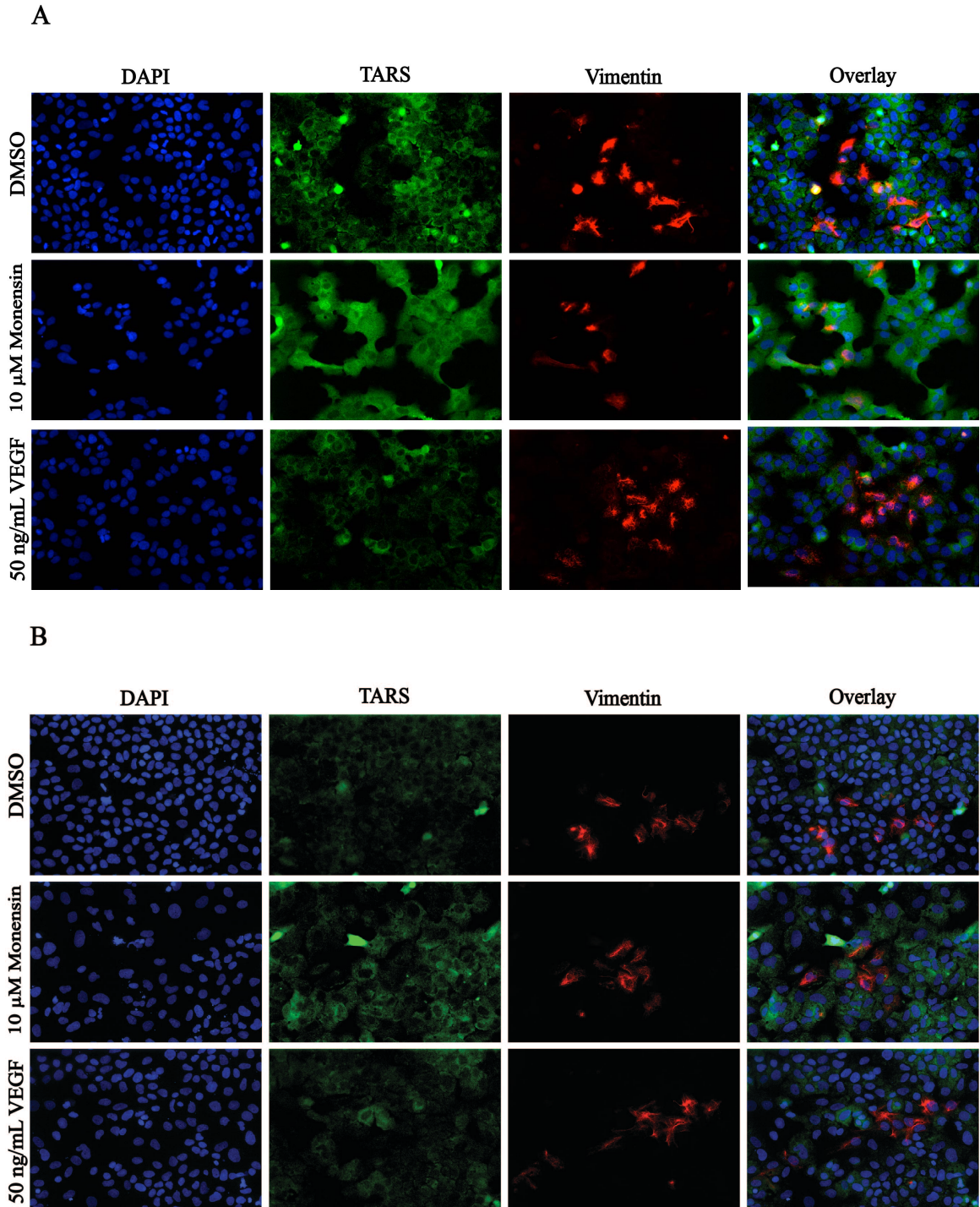


Fig. 8: Monensin-treated CaOV-3 cells have increased intracellular TARS by IMF microscopy. (A, B) CaOV-3 cells were grown on glass cover slips and treated with either 0.1% FBS (A) or 10% FBS (B) and either DMSO, 10 μ M monensin or 50 ng/mL VEGF for 18h. Cells were fixed with 10% formalin and stained with DAPI, mouse anti-TARS and rabbit anti-vimentin antibodies. DAPI, TexasRed and FITC channels were used to acquire images.

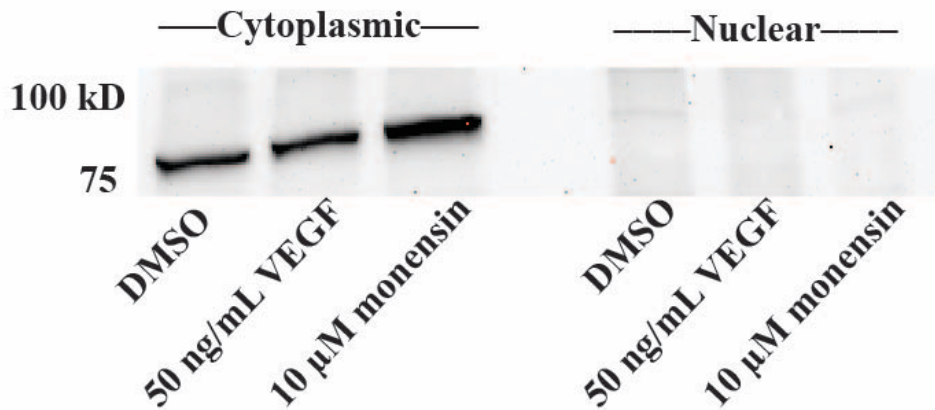


Fig. 9: TARS localizes to the cytoplasm of CaOV-3 cells. CaOV-3 cells were serum-starved and treated with DMSO, 50 ng/mL VEGF or 10 μ M monensin. Cells were lysed and nuclear and cytoplasmic lysates were separated and resolved by Western blot. A primary antibody against TARS was used. Anti- β -tubulin and anti-lamin A/C primary antibodies were used as loading control for cytoplasmic and nuclear fractions, respectively (not shown).

DNAJB9 is a member of the DNAJ protein family, which act as accessory proteins to regulate the 70 kD heat shock protein family (Hsp70) (Shen, Meunier et al. 2002).

Specifically, DNAJB9 localizes to the ER where it regulates the heat shock protein BiP, and has been found to combat cell death induced by ER stress (Shen, Meunier et al. 2002, Kurisu, Honma et al. 2003). DNAJB9 has also been found to interact with p53 protein, and act as an inhibitor of p53-induced apoptosis (Lee, Kim et al. 2015). We found that monensin caused DNAJB9 mRNA levels to increase 2-fold in CaOV-3 cells (Fig. 10A). VEGF treatment did not induce an increase in either DNAJB9 or TARS transcript levels (Figs. 10A-B). These data show that monensin is inducing ER stress, which is subsequently causing TARS transcript levels to increase.

Monensin treatment did not cause LARS transcript levels to increase (Fig. 10C), but did cause AARS transcript levels to increase 2-fold, similar to TARS transcript (Fig.

10D). VEGF treatment did not affect either LARS or AARS transcript levels. The increase in AARS transcript levels in response to monensin suggests that the synthetase transcript induction by ER stress may not be a TARS-specific response. This result could be indicative of the ARS family's role in total protein synthesis. However, LARS transcript does not increase in response to monensin treatment, and so the ER stress-induced synthetase transcript increase is not a family-wide response.

VEGF transcript levels increase 6-fold in response to monensin treatment (Fig. 10E). The increase in VEGF transcript suggests a pro-angiogenic response by CaOV-3 cells in response to monensin. It is unknown how this increase in VEGF transcript may be affecting TARS protein or transcript. However, we show that CaOV-3 cells exhibit a pro-angiogenic response that is coupled with an increase in TARS and AARS transcript levels following ER stress by monensin.

All transcript values discussed above are referring to the 0.1% FBS-treated cells. These cells were exposed to the additional stress of being treated in low serum media. Interestingly, DNAJB9 transcript levels increase slightly more in high serum-treated cells treated with monensin compared to low serum, monensin-treated cells.

These data confirm monensin is causing ER stress in CaOV-3 cells. TARS and AARS transcript levels both have a 2-fold increase in response to ER stress induced by monensin, while VEGF transcript levels increase 6-fold. Statistical significance was obtained for all monensin treated groups compared to the DMSO control within the respective serum level.

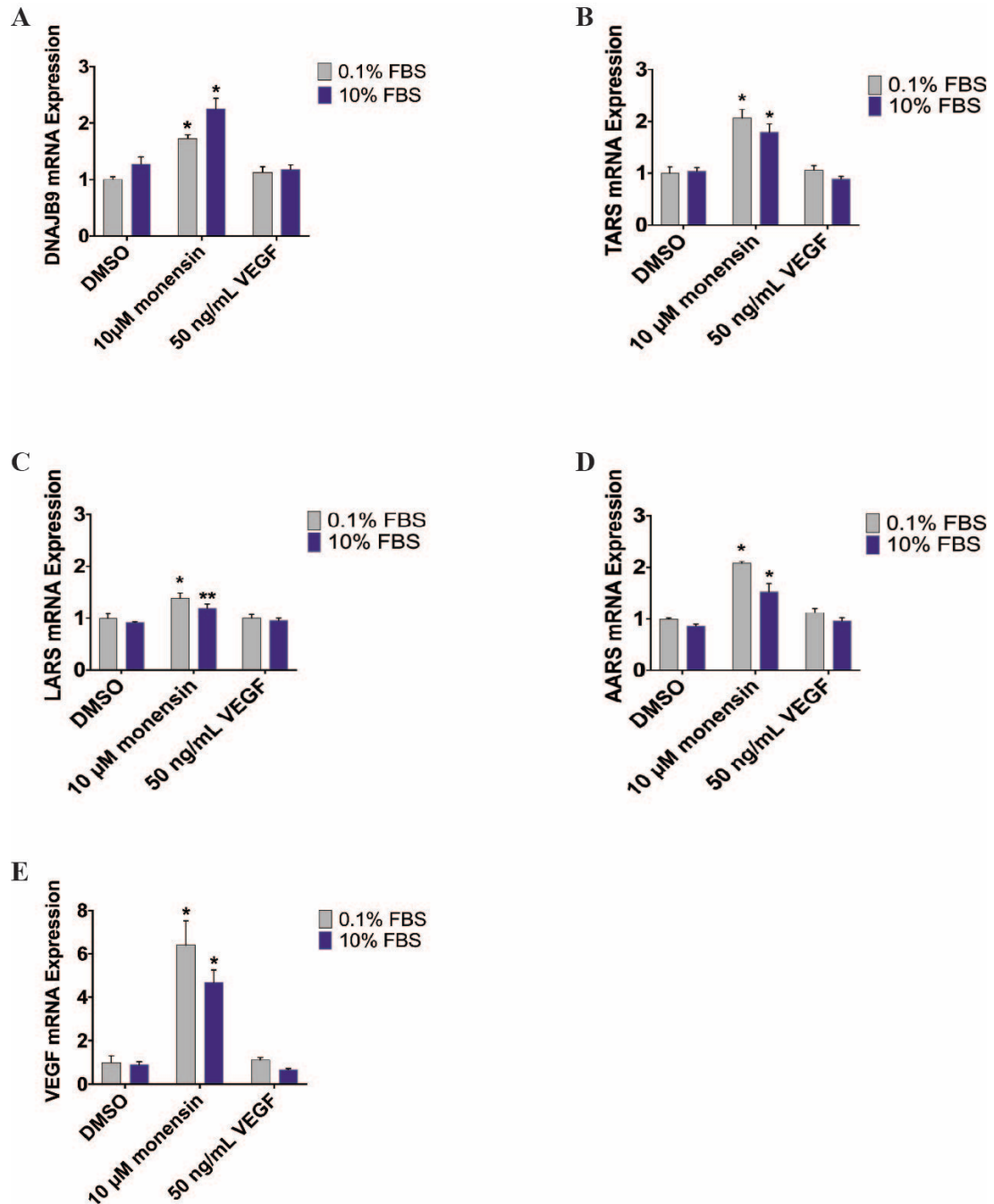


Fig. 10: Changing mRNA expression levels in CaOV-3 cells in response to ER stress.

(A-E) RT-qPCR values for DNAJB9 (A), TARS (B), LARS (C), AARS (D) and VEGF (E) were measured. CaOV-3 cells were incubated in either 0.1% or 10% FBS for 18h. In addition, cells were treated with either DMSO, 10 μM monensin or 50 ng/mL VEGF. Total RNA was extracted using a Qiagen RNeasy® Mini Kit and expression levels were determined using the $\Delta\Delta CT$ method relative to the *hprt* gene as a housekeeper. Values were normalized to 0.1% FBS, DMSO-treated cells; mean \pm SEM, n=4, *p \leq 0.0008, **p<0.015 relative to DMSO at respective [FBS] (Two-way ANOVA).

With knowledge that monensin was inducing ER stress, we next wanted to determine if titration of increasing monensin concentrations onto CaOV-3 cells would cause an increase in intracellular TARS protein that correlates with increased ER stress. CaOV-3 cells were treated with 0 μ M-10 μ M monensin with a logarithmic increase. TARS, LARS, AARS and p-eIF2 α protein levels were determined by Western blot (Figs. 11A-B). TARS protein levels increased accordingly with increasing monensin concentrations (Fig. 11C). A similar pattern of increase was observed in p-eIF2 α protein levels (Fig. 11F). These data indicate that TARS protein levels and UPR induction are correlated upon treatment with monensin, and both increase as the concentration of monensin increases. These trends did not match statistical significance, and so further trials are required to confirm our results.

LARS and AARS protein levels did not show a clear increase that corresponded to increasing monensin concentration (Figs. 11D-E). The lack of correlation between monensin concentration and LARS and AARS protein levels further suggests that the CaOV-3 cell response to ER stress by monensin at the level of synthetase proteins is TARS-specific.

TARS and p-eIF2 α protein levels both increase in CaOV-3 cells as monensin concentration increases indicating a correlation between ER stress induction and TARS protein expression. This dose-response effect was found to be TARS-specific, as LARS and AARS protein levels did not exhibit a similar monensin concentration-dependent increase. Due to the lack of statistical significance and the high error in this experiment, these conclusions are solely based on trends.

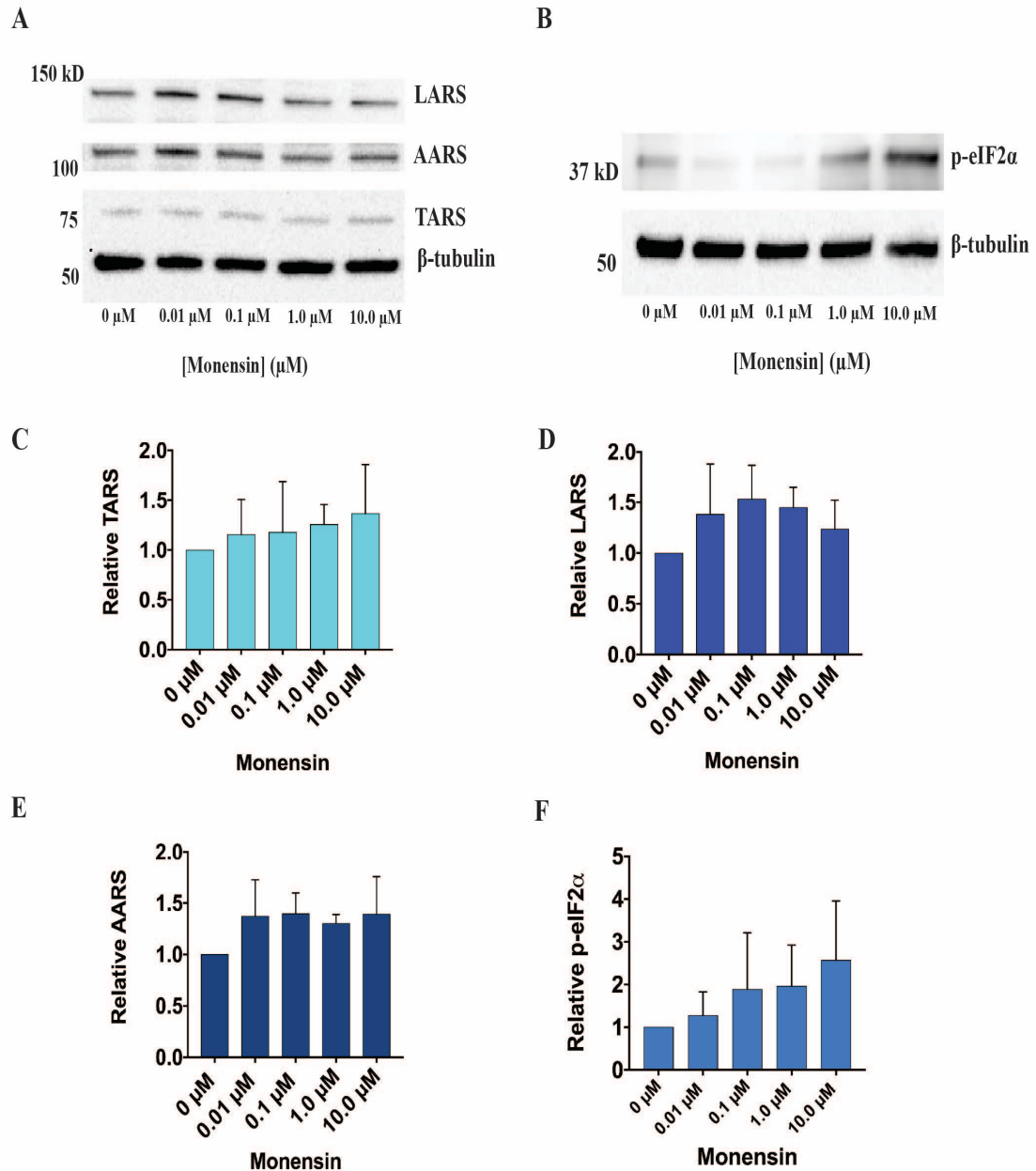


Fig. 11: TARS and p-eIF2 α protein levels increase in response to increasing monensin. CaOV-3 cells were treated in serum-free media and respective concentrations of monensin. Total cell lysates were resolved by Western blot and primary antibodies were used against TARS, LARS, AARS and p-eIF2 α . (A, B) Two representative blots are shown for TARS, LARS and AARS (A) and for p-eIF2 α (B) proteins. (C-F) TARS (C), LARS (D), AARS (E) and p-eIF2 α (F) protein levels were quantified relative to β -tubulin and normalized to 0 μ M monensin; mean \pm SEM, n=3, p>0.05 comparing experimental groups and 0 μ M monensin (Kruskal-Wallis, Dunn's multiple comparisons test).

These results were furthered by examining transcript levels in CaOV-3 cells in response to increasing monensin concentrations. TARS transcript levels increased accordingly with increasing monensin concentrations (Fig. 12B). TARS transcript levels increased 2-fold with 10 μ M monensin, which agrees with earlier RT-qPCR data (Fig. 10B). DNAJB9 transcript levels also exhibit a dose-dependent increase with increasing monensin concentration (Fig. 12A), however this increase is less pronounced than the increase in TARS. These data suggest that TARS is increasing at the transcript level as the ER stress response increases in strength.

LARS transcript levels increase following monensin treatment, however this increase does not correlate to monensin concentration (Fig. 12C). In contrast, AARS transcript levels increase accordingly with increasing monensin concentration (Fig. 12D). Similar to prior RT-qPCR results (Figs. 10B and D), TARS and AARS transcript levels in CaOV-3 cells show similar trends in response to monensin. Therefore, the ARSs seem to respond to monensin at the mRNA level differently than at the protein expression level, and this transcript response is not TARS-specific.

VEGF transcript levels show a clear increase that corresponds to increasing monensin concentrations (Fig. 12E). This furthers the argument that CaOV-3 cells become pro-angiogenic following ER stress by monensin. Following 10.0 μ M monensin treatment of CaOV-3 cells, VEGF transcript levels increase 4-fold (Fig. 12E) while TARS transcript levels increase 2-fold (Fig. 12B). Both of these increases are statistically significant. Therefore, the VEGF transcript response to monensin is more strongly induced than the TARS transcript response in CaOV-3 cells.

ER stress by monensin shows minor increase at the DNAJB9 transcript level as increasing concentrations of monensin are applied to CaOV-3 cells. TARS and AARS transcript levels increase in correlation with increasing monensin concentrations, indicating that the ARS transcript response to ER stress is likely not TARS-specific. These ARS transcript data agree with earlier results (Fig. 10). The value for TARS mRNA in CaOV-3 cells following 10 μ M monensin treatment (Fig. 12B), however, was the only synthetase transcript value that had statistical significance. The VEGF transcript levels showed a clear, dose-dependent increase in response to increasing monensin concentrations, which furthers the claim that monensin promotes a pro-angiogenic tumor microenvironment.

Next we wanted to test the effects of borrelidin, a known inhibitor of TARS and ER stress inducer, on CaOV-3 cells' protein and transcript levels (Mirando, Fang et al. 2015). CaOV-3 cells were treated with monensin, borrelidin or monensin and borrelidin, and protein and transcript levels were quantified. Monensin and borrelidin were both used at 1.0 μ M for treatments. Whole cell lysates were resolved by Western blot and probed with anti-TARS, anti-LARS and anti-AARs antibodies (Fig. 13A) and an anti-p-eIF2 α antibody (Fig. 13B).

We found that borrelidin decreased TARS protein expression compared to monensin treatment, and monensin and borrelidin treatment yielded slightly higher TARS protein expression compared to borrelidin treatment (Fig. 13C). This result confirms monensin is increasing TARS protein expression, and shows that borrelidin is suppressing TARS protein expression.

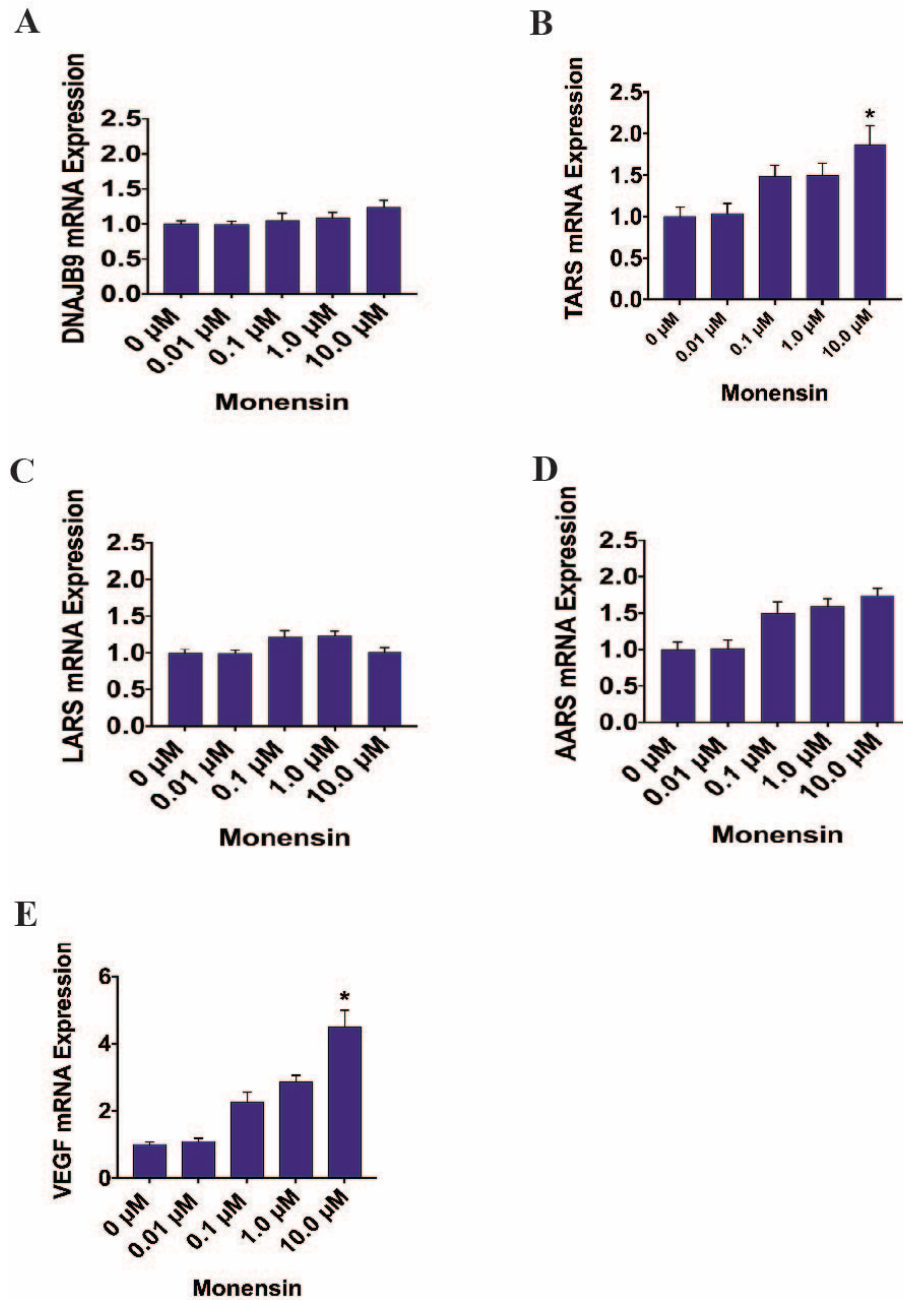


Fig. 12: TARS and VEGF transcript levels increase in response to increasing monensin. (A-E) RT-qPCR results for monensin titration onto CaOV-3 cells probing for DNAJB9 (A), TARS (B), LARS (C), AARS (D) and VEGF (E). Cells were treated with respective concentrations of monensin for 16 h in 0.1% FBS media, and total RNA was extracted using a Qiagen RNeasy® Mini Kit. Expression levels were determined using the $\Delta\Delta\text{CT}$ method relative to the *hprt* gene as a housekeeper. Values were normalized to 0 μM monensin; mean±SEM, n=3, *p<0.05 relative to 0 μM monensin (Kruskal-Wallis, Dunn's multiple comparisons test).

Borrelidin treatment of CaOV-3 cells induces the UPR as expected, which can be observed by the large spike in p-eIF2 α protein expression compared to untreated cells and monensin-treated cells (Fig. 13F). Interestingly, combined treatment with borrelidin and monensin caused a decrease in p-eIF2 α protein levels compared to the borrelidin treatment.

LARS protein levels decrease in response to borrelidin (Fig. 13D), similar to TARS protein, while AARS protein levels remain relatively unaffected in response to borrelidin treatment (Fig. 13E). Therefore, it is likely that the decrease in TARS protein expression resulting from borrelidin treatment is independent of TARS inhibition.

Borrelidin elicits a strong ER stress response, which is apparent from the dramatic increase in p-eIF2 α protein levels seen in CaOV-3 cells following borrelidin treatment. TARS protein levels decrease in response to borrelidin when compared to monensin treated cells, which suggests monensin and borrelidin are causing ER stress via separate mechanisms. No quantified protein values were statistically significant. To confirm these results more experimental trials would need to be performed. To further this experiment, we could look at how synthetases are modified in response to borrelidin treatment, and how these modifications may affect their function.

Borrelidin treatment of CaOV-3 cells had a more dramatic effect on transcript levels than it did on protein levels. Borrelidin's ER stress response was again clear at the transcript level. DNAJB9 transcript levels increased 2-fold in response to borrelidin treatment (Fig. 14A). DNAJB9 mRNA was not highly affected by monensin treatment at 1.0 μ M.

At the transcript level, borrelidin led to a 4-fold increase in TARS (Fig. 14B) and AARS (Fig. 14D), and a 2.5-fold increase in LARS (Fig. 14C) compared to the DMSO control. This shows that the cell increases transcription rates of synthetases upon ER stress induction by borrelidin. Monensin and borrelidin dual treatment yields synthetase transcripts levels that are similar to just borrelidin treatment.

VEGF transcript levels increase 11.5-fold in CaOV-3 cells in response to borrelidin treatment, and 15-fold in response to borrelidin and monensin dual treatment (Fig. 14E). This suggests that borrelidin and monensin both cause ovarian cancer cells to become pro-angiogenic intracellularly. Given the abundance of VEGF transcripts following borrelidin and monensin treatments, it could be hypothesized that the cells utilize $\alpha 6\beta 4$ integrin signaling to gain angiogenic activity under ER stress (Fig. 1).

Borrelidin induces ER stress, as is apparent by the increase in p-eIF2 α protein (Fig. 13F) and DNAJB9 transcript (Fig. 14A) in CaOV-3 cells. Similarly, monensin treatment causes an increase in p-eIF2 α protein that correlates with increasing monensin concentration (Fig. 11F). However, the mechanism of ER stress caused by borrelidin is different from that caused by monensin. Whereas monensin treatment causes an increase in TARS protein in a dose-dependent manner (Fig. 11C), borrelidin decreases TARS protein levels compared to monensin treatment (Fig. 13C). At the transcript level, both borrelidin and monensin elicit an increase in TARS transcript levels (Figs. 12B and 14B). In addition, borrelidin treatment causes a large increase in LARS and AARS transcript levels (Figs. 14C-D). Again, TARS and AARS transcript levels exhibit similar trends following cell treatment. Finally, borrelidin and monensin both induce an increase in VEGF transcript levels (Figs. 12E and 14E). Taken together, these data begin to suggest

what mechanism monensin is inducing the UPR by, and what affect that has on TARS and other synthetases.

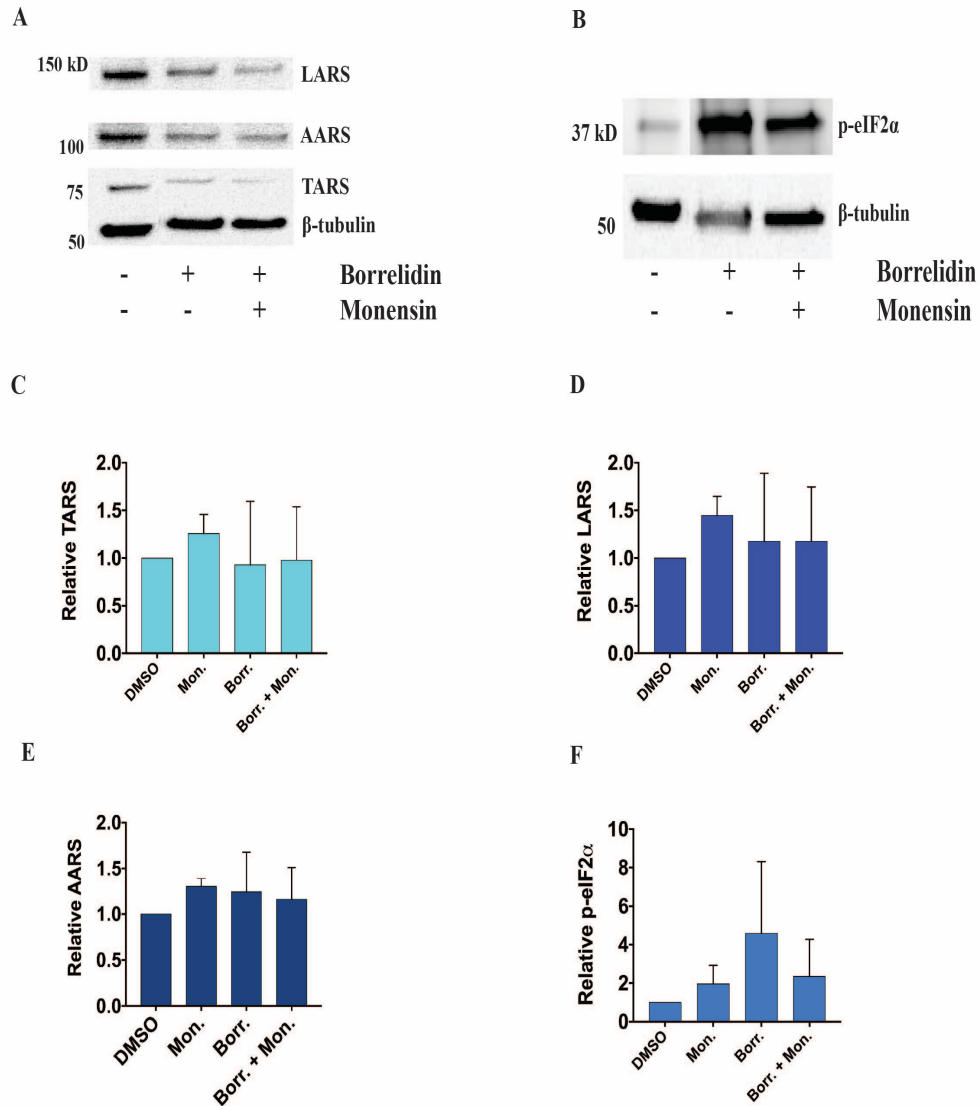


Fig. 13: Borrelidin treatment causes p-eIF2α protein to increase but not TARS protein. CaOV-3 cells were treated in serum free media and respective reagents.

Borr.=borrelidin; Mon.=monensin. DMSO served as the control treatment, and borrelidin and monensin were both used at 1.0 μM. Total cell lysates were resolved by Western blot and primary antibodies against TARS, LARS, AARS and p-eIF2α were used. (A, B) Two representative blots are shown for TARS, LARS and AARS (A) and p-eIF2α (B) proteins. (C-F) TARS (C), LARS (D), AARS (E) and p-eIF2α (F) protein levels were quantified relative to β-tubulin and normalized to DMSO. Monensin-only treated values are from the blots in Fig. 11; mean±SEM, n=3, p>0.05 comparing experimental groups and DMSO (Kruskal-Wallis, Dunn's multiple comparisons test).

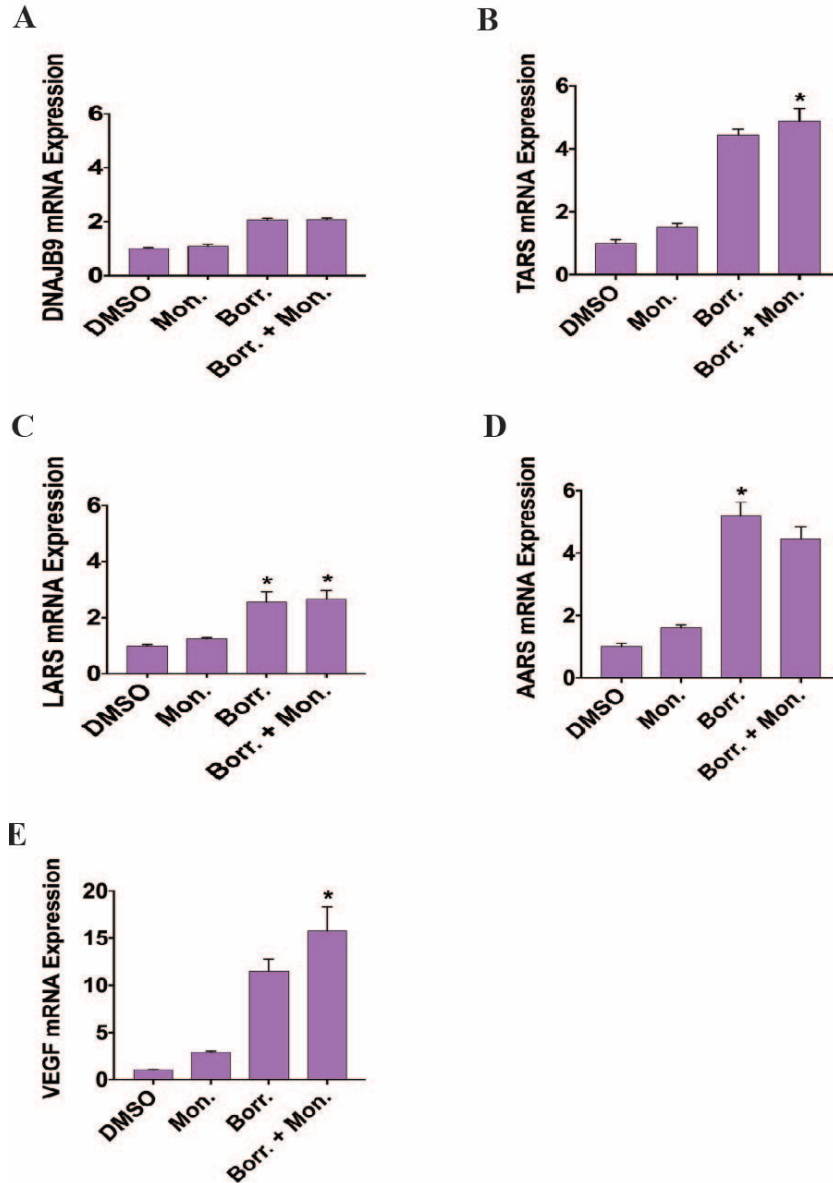


Fig. 14: Transcript levels increase in response to borrelidin and monensin treatments. (A-E) RT-qPCR results for borrelidin (Borr.) and monensin (Mon.) treatments onto CaOV-3 cells probing for DNAJB9 (A), TARS (B), LARS (C), AARS (D) and VEGF (E). Borrelidin and monensin were both used at 1.0 μ M. DMSO was used as a control treatment. Cells were treated for 16 h in 0.1% FBS media and total RNA was extracted using a Qiagen RNeasy® Mini Kit. Expression levels were determined using the $\Delta\Delta$ CT method relative to the *hprt* gene as a housekeeper. Values were normalized to DMSO; mean \pm SEM, n=3, *p<0.05 relative to DMSO (Kruskal-Wallis, Dunn's multiple comparisons test).

4.3 Conclusion

We are able to show that monensin serves as a valid experimental tool in further deciphering non-canonical functions of TARS both extracellularly and as a participant in the UPR in ovarian cancer cells. Monensin stimulates TARS secretion from CaOV-3 cells, however the mechanism of TARS secretion remains undefined. Additionally, monensin causes TARS protein and transcript levels to increase intracellularly. LARS and AARS protein levels and LARS transcript levels are affected inconsistently by monensin treatment. AARS transcript levels show a correlation to TARS transcript levels in response to monensin treatment. VEGF transcript levels are also increased significantly with monensin treatment of CaOV-3 cells. We confirm that monensin induces ER stress, and that the mechanism by which it stimulates the UPR likely differs from borrelidin UPR induction. Together these data yield insight into the role TARS plays in promotion of cancer cell survival.

CHAPTER 5: DISCUSSION AND FUTURE DIRECTIONS

5.1 Monensin as a Novel Model to Study TARS

5.1.1 Molecular Effects of Monensin

In this study we show that monensin treatment of ovarian cancer cells provides both a novel approach for studying TARS secretion, and for studying TARS expression in response to ER stress. Given the pro-angiogenic function of extracellular TARS in endothelial cells (Williams, Mirando et al. 2013), it is important to discern what molecular conditions affect TARS levels intracellularly and how TARS is being secreted. Studying TARS in a cancer model begins to expand the angiogenic potential of TARS. We provide evidence that monensin stimulates TARS secretion (Fig. 4), however the precise mechanism of secretion remains unresolved. We also show evidence that monensin promotes ER stress, and that TARS protein and transcript expression increases following monensin treatment. Although monensin is not widely found in nature, its effects on ovarian cancer cells with respect to TARS expression have yielded valuable information.

Monensin is an ionophore that disrupts the Na^+/H^+ gradient across the plasma membrane. In our experimental model we initially used monensin to increase exosome production, however the observation that monensin causes ER stress provides a clue to its other possible effect on cells. Not only has monensin been found to sensitize glioma cells to TRAIL-mediated apoptosis (Yoon, Kang et al. 2013), but monensin was also found to induce oxidative stress and apoptosis in prostate cancer cells, and to inhibit growth

through cell cycle arrest and apoptosis in lymphoma and renal carcinoma cells (Park, Seol et al. 2002, Park, Jung et al. 2003, Ketola, Vainio et al. 2010). The link to apoptosis raises concern over whether or not the detected extracellular TARS protein was a result of secretion.

Apoptotic cells have distinct changes in their morphology referred to as “apoptotic bodies” that bleb off from the cell membrane, and are ultimately engulfed and destroyed by macrophages (Elmore 2007). This event does not result in an inflammatory response. Apoptosis is different from necrosis, which is another form of cell death where the cell membrane integrity is disrupted and the cell spills its contents into the extracellular space eliciting an inflammatory response (Elmore 2007). Since monensin has been specifically linked with apoptosis and not necrosis in carcinoma cells, we conclude that the TARS increase in the cell media of cultured CaOV-3 cells was a result of secretion. However, it is important to recognize that apoptotic cells experience dysfunctional mitochondria and a homeostatic imbalance. An alternative mechanism that arose from side effects of apoptosis could have played a role in the increase in extracellular TARS protein.

5.1.2 Exosome Detection

In the present study, we were unable to confirm that the detected extracellular TARS protein was secreted via exosomal release (Fig. 5). There are many methods for exosome purification and detection, and choosing the proper one has proved challenging for many researchers. Issues surrounding exosome isolation include avoiding aggregates (more than one particle stuck together), ensuring vesicles that fall within the size range of

40-100 nm have been purified, and labeling exosomes with biomarkers for detection. One common method for purifying exosomes is by ultracentrifugation (They, Amigorena et al. 2006). Other methods include separation of samples on a density gradient or by affinity chromatography (Greening, Xu et al. 2015), These methods, however, can lead to shearing of exosomes and incomplete separation. We isolated exosomes using a polyethylene glycol (PEG)-based reagent that creates a hydrophilic environment in solution, and allows for precipitation of exosomes upon low speed centrifugation. Using volume-excluding polymers like PEG has been shown to effectively purify exosomes as aggregates (Lane, Korbie et al. 2015, Weng, Sui et al. 2016).

Currently there is little uniformity in standards for detection of exosomes. Some common methods of detection are transmission electron microscopy to actually visualize exosomes, tagging exosome-bound proteins with biomarkers or beads and detecting by flow cytometry, resolving samples by Western blot and probing for exosomal marker proteins and detection with a nanoparticle analyzer. Several of these techniques have been used to detect cancer cell-derived exosomes (Welton, Khanna et al. 2010, Peinado, Aleckovic et al. 2012). Nanoparticle detection devices are the gold standard, as they can accurately yield particle size and concentration as well as detect fluorescence.

Given the wide range of options for detecting exosomes, our original hypothesis should be revisited. The isolation technique of exosomes from CaOV-3 cells seemed to efficiently purify exosomes (Fig. 5B), however our detection method relied too heavily on immunoreactivity, which ultimately yielded inconsistent and likely inaccurate results. We were able to detect nanoparticles from CaOV-3 cells on a NanoSight (Malvern) for one trial (Table 1.A). Since we are concerned with TARS packaging in exosomes, using

the NanoSight to detect fluorescent TARS in exosome fractions would be useful as well. Exosomal release is a primary mechanism cells use to send biochemical signals to other cells, and so it remains likely that the extracellular, pro-angiogenic function of TARS is enabled by exosomal release.

5.2 Post-Translational Modifications

5.2.1 Palmitoylation

Chemical modifications of TARS may alter its localization and intracellular function, which could influence its extracellular role. Post-translational modifications (PTMs) are chemical additions to side chains of specific protein residues that alter biological function. TARS gets phosphorylated and acetylated, two common PTMs, which affects its function and localization in the cell (Choudhary, Kumar et al. 2009, Zhou, Di Palma et al. 2013). Another PTM is protein palmitoylation. Palmitoylation is the reversible, covalent attachment of a palmitic acid moiety to the side chain of cysteine residues (Aicart-Ramos, Valero et al. 2011). The reversibility of this modification enables palmitoylated proteins to localize to different areas of the cell through subcellular trafficking (Aicart-Ramos, Valero et al. 2011). This added localization function results from an increase in hydrophobicity, and ability to anchor into lipid membranes. N-Ras and H-Ras are two well-characterized proteins that utilize palmitoylation and depalmitoylation to traffic between the ER, the Golgi apparatus and the plasma membrane via vesicular transport (Linder and Deschenes 2007, Aicart-Ramos, Valero et al. 2011).

Initially we hypothesized that TARS palmitoylation facilitated its packaging into exosomes. Preliminary data testing the effects of monensin on TARS palmitoylation was inconclusive, and therefore is not shown here. Given our current hypothesis that TARS is secreted by exosomal release, testing for TARS palmitoylation would yield insight into how TARS may be packaged in exosomes. Using a Group-based prediction system algorithm that predicts protein palmitoylation sites based on protein sequence found here, <http://lipid.biocuckoo.org/index/php>, we found that TARS is likely to be palmitoylated at C137, C254 and C630. The TARS sequence was found at www.unitprot.org, Human Threonine tRNA Ligase, cytoplasmic (#P26639). By synthesizing plasmids with respective cysteine residues mutated, and transfecting these plasmids into CaOV-3 cells, we could compare WT TARS with cysteine-mutant TARS. We expect that mutating these cysteine residues would block TARS palmitoylation and subsequently would block TARS secretion in response to VEGF, TNF- α or monensin, and would inhibit the pro-angiogenic function of TARS. Of note, there is evidence that tetraspanin proteins, exosome membrane localized proteins including CD63, are palmitoylated, which influences their association with other cell surface tetraspanins (Yang, Claas et al. 2002). Post-translationally modified proteins often have increased protein-protein interactions.

5.2.2 The Ubiquitin Family of Modifications

While palmitoylation is a small PTM, ubiquitin and ubiquitin-like modifications comprise a family of large peptide PTMs that modulate many different biological processes. Modification with ubiquitin has historically been associated with targeting to the proteasome, although alternative roles for this PTM have begun to emerge (Schwartz

and Hochstrasser 2003). Additionally, several ubiquitin-like protein modifications have been uncovered. SUMOylation refers to addition of a small ubiquitin-like modifier (SUMO) peptide to lysine residues typically following cell stress (Hay 2005). SUMOylation is a highly regulated process in eukaryotes, and has been found to participate in various proliferative events including cell cycle control, transcription regulation and chromatin organization (Schwartz and Hochstrasser 2003, Hay 2005). TARS has SUMOylation sites as revealed by large scale human proteome analyses, which raises the question of what conditions would cause TARS to become SUMOylated and how would TARS protein primary and secondary functions be affected in response to SUMOylation (Becker, Barysch et al. 2013, Hendriks, Lyon et al. 2017, Lamoliatte, McManus et al. 2017).

To study TARS SUMOylation experimentally, treating human cells with MG132 would be useful. MG132 has a structure that mimics a small peptide (Fig. 15A) and inhibits protein turnover following protein synthesis through inhibition of the proteasome. In HEK293 cells, it has been reported that treatment with MG132 significantly increases protein SUMOylation including ribosomal and proteasomal elements, which get localized to the nucleus (Lamoliatte, Caron et al. 2014). MG132 also generates reactive oxygen species, and has been linked with apoptosis in tumor cells, two downstream UPR effects (Han, Moon et al. 2009, Guo and Peng 2013). The combined ability of MG132 to promote SUMOylation and stimulate maladaptive UPR responses would allow us to observe whether TARS is SUMOylated during ER stress.

We report here that TARS protein expression decreases following borrelidin treatment (Fig. 13C) and TARS transcript levels increase following borrelidin treatment

(Fig. 14B) in CaOV-3 cells. Combined, these results suggest an increase in protein turnover and a decrease in protein stability. Therefore, we believe that TARS may be ubiquitinated in response to ER stress by borrelidin. In contrast, monensin increases TARS protein (Figs. 7B and 11C) and transcript (Figs. 10B and 12B) in CaOV-3 cells. This result indicates that protein turnover rate is not increasing in response to monensin. Monensin elicits ER stress, although not as strongly as borrelidin, as revealed by p-eIF2 α induction (Fig. 13F). Therefore, if monensin is stimulating PTM of TARS, it is likely not ubiquitination. However given the induction of the UPR by monensin coupled with the increased TARS expression, it is possible that TARS gains a PTM that enables it to interact with UPR elements.

For future experiments, it would be useful to compare the effects of MG132, monensin and borrelidin (Fig. 15) treatments in CaOV-3 cells with respect to TARS protein and transcript levels and TARS PTMs. This would yield information about whether or not TARS is modified in response to ER stress, and if TARS modification is required for its involvement in the UPR.

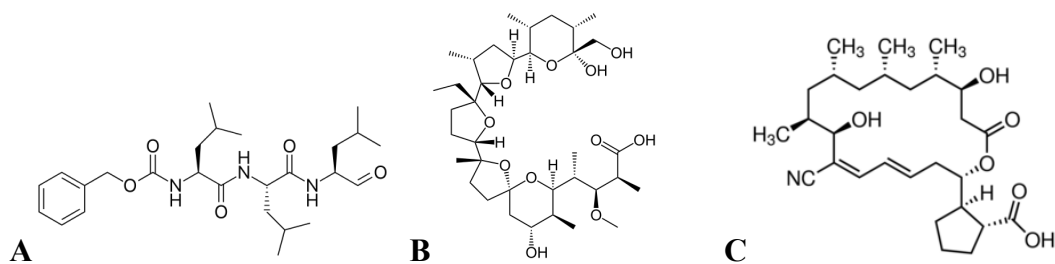


Fig. 15: Structures of MG132, Monensin and Borrelidin. (A-C) Stick structures of MG132 (A), monensin (B) and borrelidin (C).

Another PTM of interest is modification by interferon-stimulated gene 15 (ISG15). ISG15 codes for a protein that is added to peptides in response to IFN activation (Zhang and Zhang 2011). Viral infection typically causes an increase in IFN levels in the organism. This enables increased ISG15ylation of proteins, which leads to new protein-protein interactions. These new interactions increase the antiviral response, and have potential to influence protein turnover (Zhang and Zhang 2011). In various cancer cell types, TARS is modified by ISG15 following IFN treatment (Giannakopoulos, Luo et al. 2005, Zhao, Denison et al. 2005, Wong, Pung et al. 2006). Of note, WARS is also found to be ISG15ylated in these cancer cell types following IFN treatment. This furthers the role of TARS in disease, and proposes possible mechanistic intervention. Going forward, we could look at the TARS-ISG15 interaction more closely with respect to TARS localization, TARS protein interactions and UPR induction. We could also investigate whether TARS ISG15ylation affects the pro-angiogenic function of TARS. Another protein relevant to this study that gets ISG15ylated is eukaryotic translation initiation factor-4E2 (eIF4E2) (Okumura, Zou et al. 2007).

5.3 Integration of Eukaryotic Translation, ER Stress and Hypoxia

5.3.1 Hypoxic Translation Machinery

Eukaryotic translation is regulated by various initiation factors that bind to and facilitate proper mRNA translation. eIF4E is responsible for binding to and directing the ribosome to the 5'-cap of mRNA. eIF4E is inactivated by 4EBP, which constitutively binds to eIF4E and inhibits its interaction with mRNA. When 4EBP is phosphorylated it

dissociates from eIF4E, which enables eIF4E to carry out its translation initiation function. Phosphorylation of 4EBP is stimulated by the mTOR complex, which is regulated by upstream signaling cascades (Hsieh and Ruggero 2010). A recent study found that under hypoxia the mTOR pathway is inhibited in several types of cancer cells, which inhibits 4EBP phosphorylation (Uniacke, Perera et al. 2014). These carcinoma cells were found to recruit eIF4E2 to drive protein synthesis under hypoxia, which led to tumor cell survival and proliferation (Uniacke, Perera et al. 2014). Furthermore, eIF4E2 was found to form a complex with ribosomal binding protein-4 (RBM4) and hypoxia-inducible factor-2 α (Hif-2 α) under hypoxia, which binds the 5'-cap of mRNA and enables recruitment to polysomes (Uniacke, Holterman et al. 2012). Given the universal nature of a hypoxic microenvironment in tumor cells, we hypothesize that TARS is interacting with the eIF4E2/RBM4/Hif-2 α complex when cancer cells are hypoxic.

5.3.2 Does TARS Interact with Hypoxic Translation Machinery in Cancer Cells?

We tested this hypothesis in CaOV-3 cells by exposing cells to increasing time points of hypoxia, and immunoprecipitating (IP) TARS from total cell lysates to detect whether eIF4E2, RBM4 and Hif-2 α interact with TARS under hypoxia. CaOV-3 cells were exposed to 0, 4 or 16 h of hypoxia, and cells were immediately lysed once taken out of hypoxia. TARS was pulled down using magnetic Dynabeads® annealed to an anti-TARS antibody, and samples of total cell lysate (Fig. 16A), supernatant following pull down (Fig. 16B) and pelleted protein (Fig. 16C) were resolved by Western blot.

We were able to successfully pull down TARS as seen by comparison of the 16h vs. 16h no antibody control TARS blot of the pellet (Fig. 16C). However, these results do

not clearly show an interaction between TARS and eIF4E2, RBM4 and Hif-2 α that is dependent on hypoxia. In the pelleted protein Western blot (Fig. 16C), the highest levels of eIF4E2 are seen in the no antibody control, and RBM4 and Hif-2 α levels do not correlate with TARS levels at different time points of hypoxia. Supernatant protein levels (Fig. 16B) also do not decrease in accordance with TARS pull down of eIF4E2, RBM4 or Hif-2 α . Therefore, we cannot confirm at this time that TARS interacts with hypoxic translation machinery in cancer cells in a hypoxic-dependent manner.

We were able to show TARS does potentially interact with elements of the hypoxic translation machinery. Pelleted protein blots confirm that TARS, eIF4E2, RBM4 and Hif-2 α are present in samples following IP (Fig. 16C). The levels of these proteins in the pelleted samples are inconsistent with our hypothesis, however we do show presence of these four proteins across samples. One point of concern is that the highest levels of eIF4E2 protein in the pelleted samples (Fig. 16C) are observed in the no antibody control where we expected the lowest levels of eIF4E2. Therefore, our hypothesis should not be abandoned entirely, but instead we plan to alter our experimental parameters to observe this interaction.

In this IP, TARS was pulled down and TARS and hypoxic translation machinery proteins were blotted back for. Future experiments include a pull down with eIF4E2 to confirm its interaction with translational machinery. This method was not performed initially because the necessary eIF4E2 antibody was not available. It is also possible that the lack of interaction was because we did not leave the CaOV-3 cells in hypoxia for long enough. In the original study that discovered this hypoxia-induced translational functionality of eIF4E2, carcinoma cells were in hypoxia for up to 48 h (Uniacke, Perera

et al. 2014). We also plan to retest this interaction in other cell lines, cancerous and noncancerous, and to observe how borrelidin affects TARS interaction with this machinery under hypoxia. Based on this preliminary result, we will continue to pursue our hypothesis that TARS interacts with hypoxic translation machinery under hypoxia by modifying our initial experimental parameters.

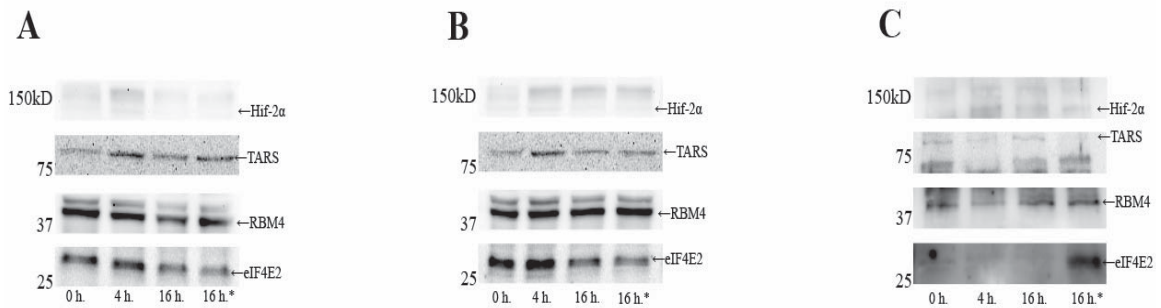


Figure 16: TARS interacts with members of the hypoxic translation machinery complex independent of hypoxia. (A-C) Immunoprecipitation of TARS from total cell lysates of CaOV-3 cells treated with increasing time in hypoxia. Samples were resolved by Western blot and antibodies against TARS, eIF4E2 (31 kD), RBM4 (40 kD) and Hif-2 α (118 kD) were used. Representative blots of total cell lysate (A), supernatant following pull down (B) and protein that was pelleted out in the IP (C) are shown. * indicates no TARS antibody was bound to the magnetic beads (no antibody control). In theory, this lane should not pull down any TARS or TARS-interacting proteins from solution.

Of note, one study found that in breast cancer cells, eIF4E is the dominant cap-binding initiation factor under both hypoxia and normoxia, and following Hif-1 α stimulation (Yi, Papadopoulos et al. 2013). The researchers also found that inhibiting the eIF4E complex under hypoxia decreases VEGF protein levels in a dose-dependent manner and has no effect on VEGF mRNA levels (Yi, Papadopoulos et al. 2013). Although this contradicts the Uniacke, Perera et al., 2014 paper, it highlights the

possibility of tissue-specific mechanisms with respect to translational control under hypoxia.

5.3.3 Comparison of Monensin and Borrelidin Effects on TARS

TARS protein's possible interaction with eIF4E2 has potential to be linked with stimulation of angiogenesis and promotion of tumor cell survival and proliferation. We speculate that upregulation of TARS protein in the hypoxic tumor microenvironment may be responsible for facilitating translation of pro-angiogenic proteins, such as VEGF. There does exist evidence supporting the role of synthetases as mediators of VEGF translation. Stimulation of human myeloid cells with IFN causes phosphorylation of EPRS at serine residues leading to the formation of the GAIT complex and subsequent binding of eIF4G, which inhibits formation of the pre-initiation complex (Jia, Yao et al. 2013, Yao and Fox 2013). In addition to its association with the GAIT complex, a truncated domain of EPRS counters translational repression by the GAIT complex creating a "translational trickle" of GAIT target proteins, including VEGF (Yao, Potdar et al. 2012, Yao, Eswarappa et al. 2015). Unpublished data from our lab confidently suggests that TARS and EPRS interact in HEK293 cells, suggesting TARS involvement in regulating translation initiation. If TARS protein is found to directly interact with eIF4E2 under hypoxic conditions, the next question would be whether or not this contributes to its pro-angiogenic function.

Extracellular TARS has a well-defined role in angiogenesis while the pro-angiogenic role of intracellular TARS remains undefined. Previous studies in our lab found that borrelidin treatment of endothelial cells increases ATF4, TARS and VEGF

transcript levels, indicating ER stress activation and pro-angiogenic function resulting from ARS inhibition. This effect was amplified under hypoxic conditions. Similarly, monensin treatment of CaOV-3 cells caused a dose-dependent increase in TARS, AARS and VEGF transcript levels (Fig. 12) and a dose-dependent increase in p-eIF2 α protein levels (Fig. 11F), which suggests a simultaneous increase in synthetase expression, promotion of a pro-angiogenic environment and ER stress induction. Given that the direct mechanism of action for monensin on ARSs and transcription/translation machinery is unknown, we can conclude that ER stress stimulation of the PERK pathway by monensin seems to be coupled with increased VEGF transcript levels and an increase in certain ARS family member's expression. Borrelidin and monensin treatments both suggest that the synthetase transcript increase is not TARS-specific in CaOV-3 cells. This is likely a survival mechanism that cells use to compensate for ER stress by increasing synthetase transcript levels, but not necessarily increasing their translation. In contrast, TARS protein levels in CaOV-3 cells increase in response to monensin (Figs. 7B and 11C) and decrease in response to borrelidin (Fig. 13C). These results were not seen with LARS or AARS protein levels. This suggests that monensin and borrelidin elicit different ER stress mechanisms, and that TARS protein plays a specific role in the ER stress response. The increase in TARS protein and VEGF transcript in response to monensin also furthers the possible angiogenic roles TARS may have intracellularly. A summary of our observed ER stress effects in CaOV-3 cells and possible integration with hypoxic translation machinery is depicted below (Fig. 17).

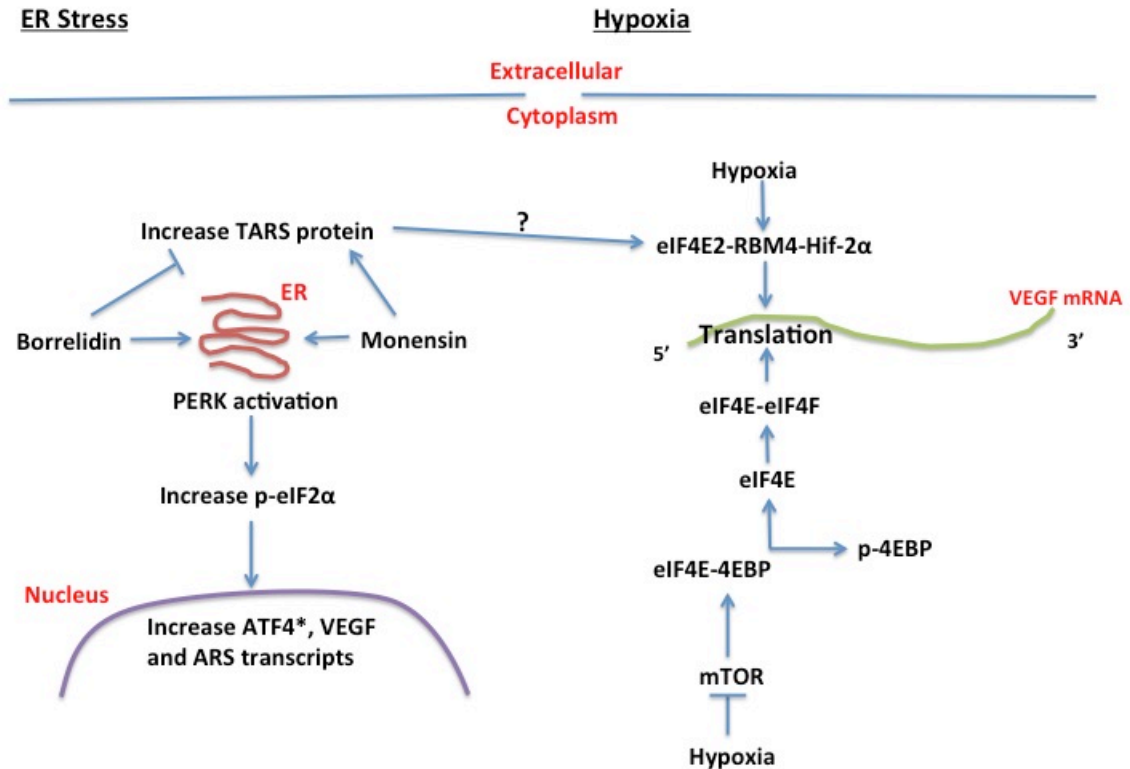


Figure 17: Summary of effects of monensin and borrelidin on ER stress and integration with hypoxic translation. The ER stress effects of borrelidin and monensin treatments on CaOV-3 cells are represented here. *ATF4 transcript increase has only been observed with borrelidin treatment of endothelial cells. Possible integration between the ER stress effects and the hypoxia translation mechanism in cancer cells is depicted. These two processes could theoretically occur in the same cell simultaneously.

5.4 Final Remarks

The ARS family is necessary for protein synthesis, and has gained attention over the past few decades due to the involvement of various family members in disease. Extracellular TARS stimulates angiogenesis and cell migration in endothelial cells, however its mechanism of secretion remains unresolved. TARS is secreted from CaOV-3

cells in response to an exosome stimulator, monensin, suggesting that exosomal release is the mechanism for TARS secretion. In addition, monensin stimulates ER stress in CaOV-3 cells, which causes an increase in TARS protein and transcript levels as well as an increase in VEGF transcript levels. TARS protein has potential to be post-translationally modified, which would affect TARS' intracellular localization and would enable new protein-protein interactions for TARS. It is possible ER stress may cause TARS to be post-translationally modified. TARS may also have increased expression in order to maintain basal translation rate of specific proteins, such as VEGF, under ER stress or hypoxia. Comparison of monensin and borrelidin treatments on various cell types has yielded insightful data about regulation of TARS expression following cell stress. Although we were unable to confirm TARS secretion by exosomal release from CaOV-3 cells, we gained invaluable information regarding conditions surrounding increased intracellular TARS expression, which allowed us to predict other non-canonical functions of TARS.

CHAPTER 6: BIBLIOGRAPHY

Abbott, J. A., C. S. Francklyn and S. M. Robey-Bond (2014). "Transfer RNA and human disease." Front Genet **5**: 158.

Adair, T. H. and J. P. Montani (2010). Angiogenesis. San Rafael (CA).

Aicart-Ramos, C., R. A. Valero and I. Rodriguez-Crespo (2011). "Protein palmitoylation and subcellular trafficking." Biochim Biophys Acta **1808**(12): 2981-2994.

Anderson, L. L., X. Mao, B. A. Scott and C. M. Crowder (2009). "Survival from hypoxia in *C. elegans* by inactivation of aminoacyl-tRNA synthetases." Science **323**(5914): 630-633.

Arnez, J. G. and D. Moras (1997). "Structural and functional considerations of the aminoacylation reaction." Trends Biochem Sci **22**(6): 211-216.

Badr, C. E., J. W. Hewett, X. O. Breakefield and B. A. Tannous (2007). "A highly sensitive assay for monitoring the secretory pathway and ER stress." PLoS One **2**(6): e571.

Baldwin, A. N. and P. Berg (1966). "Transfer ribonucleic acid-induced hydrolysis of valyladenylate bound to isoleucyl ribonucleic acid synthetase." J Biol Chem **241**(4): 839-845.

Becker, J., S. V. Barysch, S. Karaca, C. Dittner, H. H. Hsiao, M. Berriel Diaz, S. Herzig, H. Urlaub and F. Melchior (2013). "Detecting endogenous SUMO targets in mammalian cells and tissues." Nat Struct Mol Biol **20**(4): 525-531.

Bobrie, A., M. Colombo, G. Raposo and C. Thery (2011). "Exosome secretion: molecular mechanisms and roles in immune responses." Traffic **12**(12): 1659-1668.

Bradford, M. M. (1976). "A rapid and sensitive method for the quantitation of microgram quantities of protein utilizing the principle of protein-dye binding." Anal Biochem **72**: 248-254.

Choi, J. W., D. G. Kim, M. C. Park, J. Y. Um, J. M. Han, S. G. Park, E. C. Choi and S. Kim (2009). "AIMP2 promotes TNFalpha-dependent apoptosis via ubiquitin-mediated degradation of TRAF2." J Cell Sci **122**(Pt 15): 2710-2715.

Choudhary, C., C. Kumar, F. Gnad, M. L. Nielsen, M. Rehman, T. C. Walther, J. V. Olsen and M. Mann (2009). "Lysine acetylation targets protein complexes and co-regulates major cellular functions." Science **325**(5942): 834-840.

Chung, J., R. E. Bachelder, E. A. Lipscomb, L. M. Shaw and A. M. Mercurio (2002). "Integrin (alpha 6 beta 4) regulation of eIF-4E activity and VEGF translation: a survival mechanism for carcinoma cells." J Cell Biol **158**(1): 165-174.

Demay, Y., J. Perochon, S. Szuplewski, B. Mignotte and S. Gaumer (2014). "The PERK pathway independently triggers apoptosis and a Rac1/SIpr/JNK/Dilp8 signaling favoring tissue homeostasis in a chronic ER stress Drosophila model." Cell Death Dis **5**: e1452.

Dock-Bregeon, A., R. Sankaranarayanan, P. Romby, J. Caillet, M. Springer, B. Rees, C. S. Francklyn, C. Ehresmann and D. Moras (2000). "Transfer RNA-mediated editing in threonyl-tRNA synthetase. The class II solution to the double discrimination problem." Cell **103**(6): 877-884.

Duffy, A. M., D. J. Bouchier-Hayes and J. H. Harmey Vascular Endothelial Growth Factor (VEGF) and Its Role in Non-Endothelial Cells: Autocrine Signalling by VEGF.

Elmore, S. (2007). "Apoptosis: a review of programmed cell death." Toxicol Pathol **35**(4): 495-516.

Eriksson, J. E., T. Dechat, B. Grin, B. Helfand, M. Mendez, H. M. Pallari and R. D. Goldman (2009). "Introducing intermediate filaments: from discovery to disease." J Clin Invest **119**(7): 1763-1771.

Fersht, A. R. and C. Dingwall (1979). "Evidence for the double-sieve editing mechanism in protein synthesis. Steric exclusion of isoleucine by valyl-tRNA synthetases." Biochemistry **18**(12): 2627-2631.

Fersht, A. R. and M. M. Kaethner (1976). "Enzyme hyperspecificity. Rejection of threonine by the valyl-tRNA synthetase by misacylation and hydrolytic editing." Biochemistry **15**(15): 3342-3346.

Forus, A., V. A. Florenes, G. M. Maelandsmo, O. Fodstad and O. Myklebost (1994). "The protooncogene CHOP/GADD153, involved in growth arrest and DNA damage response, is amplified in a subset of human sarcomas." Cancer Genet Cytogenet **78**(2): 165-171.

Gercel-Taylor, C., S. Atay, R. H. Tullis, M. Kesimer and D. D. Taylor (2012). "Nanoparticle analysis of circulating cell-derived vesicles in ovarian cancer patients." Anal Biochem **428**(1): 44-53.

Ghanipour, A., K. Jirstrom, F. Ponten, B. Glimelius, L. Pahlman and H. Birgisson (2009). "The prognostic significance of tryptophanyl-tRNA synthetase in colorectal cancer." Cancer Epidemiol Biomarkers Prev **18**(11): 2949-2956.

Giannakopoulos, N. V., J. K. Luo, V. Papov, W. Zou, D. J. Lenschow, B. S. Jacobs, E. C. Borden, J. Li, H. W. Virgin and D. E. Zhang (2005). "Proteomic identification of proteins conjugated to ISG15 in mouse and human cells." Biochem Biophys Res Commun **336**(2): 496-506.

Giege, R., M. Sissler and C. Florentz (1998). "Universal rules and idiosyncratic features in tRNA identity." Nucleic Acids Res **26**(22): 5017-5035.

Greening, D. W., R. Xu, H. Ji, B. J. Tauro and R. J. Simpson (2015). "A protocol for exosome isolation and characterization: evaluation of ultracentrifugation, density-gradient separation, and immunoaffinity capture methods." Methods Mol Biol **1295**: 179-209.

Guo, B. B., S. A. Bellingham and A. F. Hill (2016). "Stimulating the Release of Exosomes Increases the Intercellular Transfer of Prions." J Biol Chem **291**(10): 5128-5137.

Guo, N. and Z. Peng (2013). "MG132, a proteasome inhibitor, induces apoptosis in tumor cells." Asia Pac J Clin Oncol **9**(1): 6-11.

Hamanaka, R. B., B. S. Bennett, S. B. Cullinan and J. A. Diehl (2005). "PERK and GCN2 contribute to eIF2alpha phosphorylation and cell cycle arrest after activation of the unfolded protein response pathway." Mol Biol Cell **16**(12): 5493-5501.

Han, J., S. H. Back, J. Hur, Y. H. Lin, R. Gildersleeve, J. Shan, C. L. Yuan, D. Krokowski, S. Wang, M. Hatzoglou, M. S. Kilberg, M. A. Sartor and R. J. Kaufman

(2013). "ER-stress-induced transcriptional regulation increases protein synthesis leading to cell death." Nat Cell Biol **15**(5): 481-490.

Han, J. M., B. J. Park, S. G. Park, Y. S. Oh, S. J. Choi, S. W. Lee, S. K. Hwang, S. H. Chang, M. H. Cho and S. Kim (2008). "AIMP2/p38, the scaffold for the multi-tRNA synthetase complex, responds to genotoxic stresses via p53." Proc Natl Acad Sci U S A **105**(32): 11206-11211.

Han, Y. H., H. J. Moon, B. R. You and W. H. Park (2009). "The effect of MG132, a proteasome inhibitor on HeLa cells in relation to cell growth, reactive oxygen species and GSH." Oncol Rep **22**(1): 215-221.

Harding, H. P., I. Novoa, Y. Zhang, H. Zeng, R. Wek, M. Schapira and D. Ron (2000). "Regulated translation initiation controls stress-induced gene expression in mammalian cells." Mol Cell **6**(5): 1099-1108.

Hay, R. T. (2005). "SUMO: a history of modification." Mol Cell **18**(1): 1-12.

Hendriks, I. A., D. Lyon, C. Young, L. J. Jensen, A. C. Vertegaal and M. L. Nielsen (2017). "Site-specific mapping of the human SUMO proteome reveals co-modification with phosphorylation." Nat Struct Mol Biol **24**(3): 325-336.

Hetz, C. (2012). "The unfolded protein response: controlling cell fate decisions under ER stress and beyond." Nat Rev Mol Cell Biol **13**(2): 89-102.

Hoagland, M. B., M. L. Stephenson, J. F. Scott, L. I. Hecht and P. C. Zamecnik (1958). "A soluble ribonucleic acid intermediate in protein synthesis." J Biol Chem **231**(1): 241-257.

Hsieh, A. C. and D. Ruggero (2010). "Targeting eukaryotic translation initiation factor 4E (eIF4E) in cancer." Clin Cancer Res **16**(20): 4914-4920.

Ibba, M., H. D. Becker, C. Stathopoulos, D. L. Tumbula and D. Soll (2000). "The adaptor hypothesis revisited." Trends Biochem Sci **25**(7): 311-316.

Jakubowski, H. and E. Goldman (1992). "Editing of errors in selection of amino acids for protein synthesis." Microbiol Rev **56**(3): 412-429.

Jia, J., P. Yao, A. Arif and P. L. Fox (2013). "Regulation and dysregulation of 3'UTR-mediated translational control." Curr Opin Genet Dev **23**(1): 29-34.

Jordanova, A., J. Irobi, F. P. Thomas, P. Van Dijck, K. Meerschaert, M. Dewil, I. Dierick, A. Jacobs, E. De Vriendt, V. Guerguelcheva, C. V. Rao, I. Tournev, F. A. Gondim, M. D'Hooghe, V. Van Gerwen, P. Callaerts, L. Van Den Bosch, J. P. Timmermans, W. Robberecht, J. Gettemans, J. M. Thevelein, P. De Jonghe, I. Kremensky and V. Timmerman (2006). "Disrupted function and axonal distribution of mutant tyrosyl-tRNA synthetase in dominant intermediate Charcot-Marie-Tooth neuropathy." Nat Genet **38**(2): 197-202.

Kalidas, S., I. Cestari, S. Monnerat, Q. Li, S. Regmi, N. Hasle, M. Labaied, M. Parsons, K. Stuart and M. A. Phillips (2014). "Genetic validation of aminoacyl-tRNA synthetases as drug targets in *Trypanosoma brucei*." Eukaryot Cell **13**(4): 504-516.

Ketola, K., P. Vainio, V. Fey, O. Kallioniemi and K. Iljin (2010). "Monensin is a potent inducer of oxidative stress and inhibitor of androgen signaling leading to apoptosis in prostate cancer cells." Mol Cancer Ther **9**(12): 3175-3185.

Kim, S., S. You and D. Hwang (2011). "Aminoacyl-tRNA synthetases and tumorigenesis: more than housekeeping." Nat Rev Cancer **11**(10): 708-718.

King, H. W., M. Z. Michael and J. M. Gleadle (2012). "Hypoxic enhancement of exosome release by breast cancer cells." BMC Cancer **12**: 421.

Konovalova, S. and H. Tyynismaa (2013). "Mitochondrial aminoacyl-tRNA synthetases in human disease." Mol Genet Metab **108**(4): 206-211.

Kurusu, J., A. Honma, H. Miyajima, S. Kondo, M. Okumura and K. Imaizumi (2003). "MDG1/ERdj4, an ER-resident DnaJ family member, suppresses cell death induced by ER stress." Genes Cells **8**(2): 189-202.

Kurland, C. G. and S. G. Andersson (2000). "Origin and evolution of the mitochondrial proteome." Microbiol Mol Biol Rev **64**(4): 786-820.

Kushner, J. P., D. Boll, J. Quagliana and S. Dickman (1976). "Elevated methionine-tRNA synthetase activity in human colon cancer." Proc Soc Exp Biol Med **153**(2): 273-276.

- Labirua, A. and I. E. Lundberg (2010). "Interstitial lung disease and idiopathic inflammatory myopathies: progress and pitfalls." Curr Opin Rheumatol **22**(6): 633-638.
- Lamoliatte, F., D. Caron, C. Durette, L. Mahrouche, M. A. Maroui, O. Caron-Lizotte, E. Bonneil, M. K. Chelbi-Alix and P. Thibault (2014). "Large-scale analysis of lysine SUMOylation by SUMO remnant immunoaffinity profiling." Nat Commun **5**: 5409.
- Lamoliatte, F., F. P. McManus, G. Maarifi, M. K. Chelbi-Alix and P. Thibault (2017). "Uncovering the SUMOylation and ubiquitylation crosstalk in human cells using sequential peptide immunopurification." Nat Commun **8**: 14109.
- Lane, R. E., D. Korbie, W. Anderson, R. Vaidyanathan and M. Trau (2015). "Analysis of exosome purification methods using a model liposome system and tunable-resistive pulse sensing." Sci Rep **5**: 7639.
- Lee, H. J., J. M. Kim, K. H. Kim, J. I. Heo, S. J. Kwak and J. A. Han (2015). "Genotoxic stress/p53-induced DNAJB9 inhibits the pro-apoptotic function of p53." Cell Death Differ **22**(1): 86-95.
- Lee, J. W., K. Beebe, L. A. Nangle, J. Jang, C. M. Longo-Guess, S. A. Cook, M. T. Davison, J. P. Sundberg, P. Schimmel and S. L. Ackerman (2006). "Editing-defective tRNA synthetase causes protein misfolding and neurodegeneration." Nature **443**(7107): 50-55.
- Liang, B., P. Peng, S. Chen, L. Li, M. Zhang, D. Cao, J. Yang, H. Li, T. Gui, X. Li and K. Shen (2013). "Characterization and proteomic analysis of ovarian cancer-derived exosomes." J Proteomics **80**: 171-182.
- Lin, J. H., H. Li, D. Yasumura, H. R. Cohen, C. Zhang, B. Panning, K. M. Shokat, M. M. Lavail and P. Walter (2007). "IRE1 signaling affects cell fate during the unfolded protein response." Science **318**(5852): 944-949.
- Linder, M. E. and R. J. Deschenes (2007). "Palmitoylation: policing protein stability and traffic." Nat Rev Mol Cell Biol **8**(1): 74-84.
- Marintchev, A. (2012). "Fidelity and quality control in gene expression. Preface." Adv Protein Chem Struct Biol **86**: ix.

- Martinis, S. A. and M. T. Boniecki (2010). "The balance between pre- and post-transfer editing in tRNA synthetases." FEBS Lett **584**(2): 455-459.
- Melone, M. A., A. Tessa, S. Petrini, G. Lus, S. Sampaolo, G. di Fede, F. M. Santorelli and R. Cotrufo (2004). "Revelation of a new mitochondrial DNA mutation (G12147A) in a MELAS/MERFF phenotype." Arch Neurol **61**(2): 269-272.
- Meral, I., W. Hsu and F. B. Hembrough (2002). "Digoxin- and monensin-induced changes of intracellular Ca²⁺ concentration in isolated guinea-pig ventricular myocyte." J Vet Med A Physiol Pathol Clin Med **49**(6): 329-333.
- Miller, F. W., K. A. Waite, T. Biswas and P. H. Plotz (1990). "The role of an autoantigen, histidyl-tRNA synthetase, in the induction and maintenance of autoimmunity." Proc Natl Acad Sci U S A **87**(24): 9933-9937.
- Mirando, A. C., P. Fang, T. F. Williams, L. C. Baldor, A. K. Howe, A. M. Ebert, B. Wilkinson, K. M. Lounsbury, M. Guo and C. S. Francklyn (2015). "Aminoacyl-tRNA synthetase dependent angiogenesis revealed by a bioengineered macrolide inhibitor." Sci Rep **5**: 13160.
- Mirando, A. C., C. S. Francklyn and K. M. Lounsbury (2014). "Regulation of angiogenesis by aminoacyl-tRNA synthetases." Int J Mol Sci **15**(12): 23725-23748.
- Mollenhauer, H. H., D. J. Morre and L. D. Rowe (1990). "Alteration of intracellular traffic by monensin; mechanism, specificity and relationship to toxicity." Biochim Biophys Acta **1031**(2): 225-246.
- Munoz-Chapuli, R., A. R. Quesada and M. Angel Medina (2004). "Angiogenesis and signal transduction in endothelial cells." Cell Mol Life Sci **61**(17): 2224-2243.
- Notman, R., M. Noro, B. O'Malley and J. Anwar (2006). "Molecular basis for dimethylsulfoxide (DMSO) action on lipid membranes." J Am Chem Soc **128**(43): 13982-13983.
- Nureki, O., D. G. Vassylyev, M. Tateno, A. Shimada, T. Nakama, S. Fukai, M. Konno, T. L. Hendrickson, P. Schimmel and S. Yokoyama (1998). "Enzyme structure with two catalytic sites for double-sieve selection of substrate." Science **280**(5363): 578-582.

Okumura, F., W. Zou and D. E. Zhang (2007). "ISG15 modification of the eIF4E cognate 4EHP enhances cap structure-binding activity of 4EHP." Genes Dev **21**(3): 255-260.

Osowski, C. M. and F. Urano (2011). "Measuring ER stress and the unfolded protein response using mammalian tissue culture system." Methods Enzymol **490**: 71-92.

Park, W. H., C. W. Jung, J. O. Park, K. Kim, W. S. Kim, Y. H. Im, M. H. Lee, W. K. Kang and K. Park (2003). "Monensin inhibits the growth of renal cell carcinoma cells via cell cycle arrest or apoptosis." Int J Oncol **22**(4): 855-860.

Park, W. H., J. G. Seol, E. S. Kim, W. K. Kang, Y. H. Im, C. W. Jung, B. K. Kim and Y. Y. Lee (2002). "Monensin-mediated growth inhibition in human lymphoma cells through cell cycle arrest and apoptosis." Br J Haematol **119**(2): 400-407.

Peinado, H., M. Aleckovic, S. Lavotshkin, I. Matei, B. Costa-Silva, G. Moreno-Bueno, M. Hergueta-Redondo, C. Williams, G. Garcia-Santos, C. Ghajar, A. Nitadori-Hoshino, C. Hoffman, K. Badal, B. A. Garcia, M. K. Callahan, J. Yuan, V. R. Martins, J. Skog, R. N. Kaplan, M. S. Brady, J. D. Wolchok, P. B. Chapman, Y. Kang, J. Bromberg and D. Lyden (2012). "Melanoma exosomes educate bone marrow progenitor cells toward a pro-metastatic phenotype through MET." Nat Med **18**(6): 883-891.

Pols, M. S. and J. Klumperman (2009). "Trafficking and function of the tetraspanin CD63." Exp Cell Res **315**(9): 1584-1592.

Ray, P. S., A. Arif and P. L. Fox (2007). "Macromolecular complexes as depots for releasable regulatory proteins." Trends Biochem Sci **32**(4): 158-164.

Ray, P. S. and P. L. Fox (2007). "A post-transcriptional pathway represses monocyte VEGF-A expression and angiogenic activity." EMBO J **26**(14): 3360-3372.

Sampath, P., B. Mazumder, V. Seshadri, C. A. Gerber, L. Chavatte, M. Kinter, S. M. Ting, J. D. Dignam, S. Kim, D. M. Driscoll and P. L. Fox (2004). "Noncanonical function of glutamyl-prolyl-tRNA synthetase: gene-specific silencing of translation." Cell **119**(2): 195-208.

Sankaranarayanan, R. and D. Moras (2001). "The fidelity of the translation of the genetic code." Acta Biochim Pol **48**(2): 323-335.

Satelli, A. and S. Li (2011). "Vimentin in cancer and its potential as a molecular target for cancer therapy." Cell Mol Life Sci **68**(18): 3033-3046.

Savina, A., M. Furlan, M. Vidal and M. I. Colombo (2003). "Exosome release is regulated by a calcium-dependent mechanism in K562 cells." J Biol Chem **278**(22): 20083-20090.

Schwartz, D. C. and M. Hochstrasser (2003). "A superfamily of protein tags: ubiquitin, SUMO and related modifiers." Trends Biochem Sci **28**(6): 321-328.

Shen, Y., L. Meunier and L. M. Hendershot (2002). "Identification and characterization of a novel endoplasmic reticulum (ER) DnaJ homologue, which stimulates ATPase activity of BiP in vitro and is induced by ER stress." J Biol Chem **277**(18): 15947-15956.

Sidhu, A., J. R. Miller, A. Tripathi, D. M. Garshott, A. L. Brownell, D. J. Chiego, C. Arevang, Q. Zeng, L. C. Jackson, S. A. Bechler, M. U. Callaghan, G. H. Yoo, S. Sethi, H. S. Lin, J. H. Callaghan, G. Tamayo-Castillo, D. H. Sherman, R. J. Kaufman and A. M. Fribley (2015). "Borrelidin Induces the Unfolded Protein Response in Oral Cancer Cells and Chop-Dependent Apoptosis." ACS Med Chem Lett **6**(11): 1122-1127.

Silvestri, G., C. T. Moraes, S. Shanske, S. J. Oh and S. DiMauro (1992). "A new mtDNA mutation in the tRNA(Lys) gene associated with myoclonic epilepsy and ragged-red fibers (MERRF)." Am J Hum Genet **51**(6): 1213-1217.

Suzuki, T., A. Nagao and T. Suzuki (2011). "Human mitochondrial tRNAs: biogenesis, function, structural aspects, and diseases." Annu Rev Genet **45**: 299-329.

Szymanski, M., M. A. Deniziak and J. Barciszewski (2001). "Aminoacyl-tRNA synthetases database." Nucleic Acids Res **29**(1): 288-290.

They, C., S. Amigorena, G. Raposo and A. Clayton (2006). "Isolation and characterization of exosomes from cell culture supernatants and biological fluids." Curr Protoc Cell Biol **Chapter 3**: Unit 3 22.

Tsuru, A., Y. Imai, M. Saito and K. Kohno (2016). "Novel mechanism of enhancing IRE1 α -XBP1 signalling via the PERK-ATF4 pathway." Sci Rep **6**: 24217.

Tzima, E., J. S. Reader, M. Irani-Tehrani, K. L. Ewalt, M. A. Schwartz and P. Schimmel (2003). "Biologically active fragment of a human tRNA synthetase inhibits fluid shear stress-activated responses of endothelial cells." Proc Natl Acad Sci U S A **100**(25): 14903-14907.

Tzima, E. and P. Schimmel (2006). "Inhibition of tumor angiogenesis by a natural fragment of a tRNA synthetase." Trends Biochem Sci **31**(1): 7-10.

Ubeda, M., M. Schmitt-Ney, J. Ferrer and J. F. Habener (1999). "CHOP/GADD153 and methionyl-tRNA synthetase (MetRS) genes overlap in a conserved region that controls mRNA stability." Biochem Biophys Res Commun **262**(1): 31-38.

Uniacke, J., C. E. Holterman, G. Lachance, A. Franovic, M. D. Jacob, M. R. Fabian, J. Payette, M. Holcik, A. Pause and S. Lee (2012). "An oxygen-regulated switch in the protein synthesis machinery." Nature **486**(7401): 126-129.

Uniacke, J., J. K. Perera, G. Lachance, C. B. Francisco and S. Lee (2014). "Cancer cells exploit eIF4E2-directed synthesis of hypoxia response proteins to drive tumor progression." Cancer Res **74**(5): 1379-1389.

van Berge, L., S. Dooves, C. G. van Berkel, E. Polder, M. S. van der Knaap and G. C. Scheper (2012). "Leukoencephalopathy with brain stem and spinal cord involvement and lactate elevation is associated with cell-type-dependent splicing of mtAspRS mRNA." Biochem J **441**(3): 955-962.

Walter, P. and D. Ron (2011). "The unfolded protein response: from stress pathway to homeostatic regulation." Science **334**(6059): 1081-1086.

Wang, F., Z. Xu, J. Zhou, W. S. Lo, C. F. Lau, L. A. Nangle, X. L. Yang, M. Zhang and P. Schimmel (2013). "Regulated capture by exosomes of mRNAs for cytoplasmic tRNA synthetases." J Biol Chem **288**(41): 29223-29228.

Wang, M. and R. J. Kaufman (2016). "Protein misfolding in the endoplasmic reticulum as a conduit to human disease." Nature **529**(7586): 326-335.

Wek, S. A., S. Zhu and R. C. Wek (1995). "The histidyl-tRNA synthetase-related sequence in the eIF-2 alpha protein kinase GCN2 interacts with tRNA and is required for activation in response to starvation for different amino acids." Mol Cell Biol **15**(8): 4497-4506.

Wellman, T. L., M. Eckenstein, C. Wong, M. Rincon, T. Ashikaga, S. L. Mount, C. S. Francklyn and K. M. Lounsbury (2014). "Threonyl-tRNA synthetase overexpression correlates with angiogenic markers and progression of human ovarian cancer." BMC Cancer **14**: 620.

Welton, J. L., S. Khanna, P. J. Giles, P. Brennan, I. A. Brewis, J. Staffurth, M. D. Mason and A. Clayton (2010). "Proteomics analysis of bladder cancer exosomes." Mol Cell Proteomics **9**(6): 1324-1338.

Weng, Y., Z. Sui, Y. Shan, Y. Hu, Y. Chen, L. Zhang and Y. Zhang (2016). "Effective isolation of exosomes with polyethylene glycol from cell culture supernatant for in-depth proteome profiling." Analyst **141**(15): 4640-4646.

Williams, T. F., A. C. Mirando, B. Wilkinson, C. S. Francklyn and K. M. Lounsbury (2013). "Secreted Threonyl-tRNA synthetase stimulates endothelial cell migration and angiogenesis." Sci Rep **3**: 1317.

Wong, J. J., Y. F. Pung, N. S. Sze and K. C. Chin (2006). "HERC5 is an IFN-induced HECT-type E3 protein ligase that mediates type I IFN-induced ISGylation of protein targets." Proc Natl Acad Sci U S A **103**(28): 10735-10740.

Yang, X., C. Claas, S. K. Kraeft, L. B. Chen, Z. Wang, J. A. Kreidberg and M. E. Hemler (2002). "Palmitoylation of tetraspanin proteins: modulation of CD151 lateral interactions, subcellular distribution, and integrin-dependent cell morphology." Mol Biol Cell **13**(3): 767-781.

Yao, P., S. M. Eswarappa and P. L. Fox (2015). "Translational control mechanisms in angiogenesis and vascular biology." Curr Atheroscler Rep **17**(5): 506.

Yao, P. and P. L. Fox (2013). "Aminoacyl-tRNA synthetases in medicine and disease." EMBO Mol Med **5**(3): 332-343.

Yao, P., A. A. Potdar, A. Arif, P. S. Ray, R. Mukhopadhyay, B. Willard, Y. Xu, J. Yan, G. M. Saidel and P. L. Fox (2012). "Coding region polyadenylation generates a truncated tRNA synthetase that counters translation repression." Cell **149**(1): 88-100.

Yi, T., E. Papadopoulos, P. R. Hagner and G. Wagner (2013). "Hypoxia-inducible factor-1alpha (HIF-1alpha) promotes cap-dependent translation of selective mRNAs through

up-regulating initiation factor eIF4E1 in breast cancer cells under hypoxia conditions." J Biol Chem **288**(26): 18732-18742.

Yoon, M. J., Y. J. Kang, I. Y. Kim, E. H. Kim, J. A. Lee, J. H. Lim, T. K. Kwon and K. S. Choi (2013). "Monensin, a polyether ionophore antibiotic, overcomes TRAIL resistance in glioma cells via endoplasmic reticulum stress, DR5 upregulation and c-FLIP downregulation." Carcinogenesis **34**(8): 1918-1928.

Yoshida, H., T. Matsui, A. Yamamoto, T. Okada and K. Mori (2001). "XBP1 mRNA is induced by ATF6 and spliced by IRE1 in response to ER stress to produce a highly active transcription factor." Cell **107**(7): 881-891.

Zamecnik, P. C. and E. B. Keller (1954). "Relation between phosphate energy donors and incorporation of labeled amino acids into proteins." J Biol Chem **209**(1): 337-354.

Zhang, D. and D. E. Zhang (2011). "Interferon-stimulated gene 15 and the protein ISGylation system." J Interferon Cytokine Res **31**(1): 119-130.

Zhao, C., C. Denison, J. M. Huibregtse, S. Gygi and R. M. Krug (2005). "Human ISG15 conjugation targets both IFN-induced and constitutively expressed proteins functioning in diverse cellular pathways." Proc Natl Acad Sci U S A **102**(29): 10200-10205.

Zhou, H., S. Di Palma, C. Preisinger, M. Peng, A. N. Polat, A. J. Heck and S. Mohammed (2013). "Toward a comprehensive characterization of a human cancer cell phosphoproteome." J Proteome Res **12**(1): 260-271.

Zhou, J. J., F. Wang, Z. Xu, W. S. Lo, C. F. Lau, K. P. Chiang, L. A. Nangle, M. A. Ashlock, J. D. Mendlein, X. L. Yang, M. Zhang and P. Schimmel (2014). "Secreted histidyl-tRNA synthetase splice variants elaborate major epitopes for autoantibodies in inflammatory myositis." J Biol Chem **289**(28): 19269-19275.

CHAPTER 7: APPENDIX

Table A.1: NanoSight particle analysis of exosome-precipitated samples from CaOV-3 cells.

	Exosome-Depleted Media	Control	10 μM monensin	50 ng/mL VEGF
Mean Particle Size \pm Std. Error (nm)	96.4 \pm 1.7	138.5 \pm 3.0	135.2 \pm 9.2	117.6 \pm 6.5
Mode Particle Size \pm Std. Error (nm)	99.6 \pm 16.7	98.1 \pm 4.7	86.0 \pm 7.1	83.7 \pm 6.5
Std. Dev. \pm Std. Error (nm)	24.4 \pm 1.7	72.4 \pm 5.4	68.8 \pm 10.2	52.5 \pm 9.1
Concentration \pm Std. Error (particles/mL)	1.21x10 ⁸ \pm 8.30 x 10 ⁶	6.07x10 ⁸ \pm 4.27x10 ⁷	5.95x10 ⁸ \pm 6.08x10 ⁷	6.74x10 ⁸ \pm 1.49x10 ⁷

Cell media was collected and exosomes were precipitated out of solution using ExoQuick-TC™. A sample of exosome-depleted media was precipitated as a negative control. Pelleted exosomes were resuspended in clean PBS, and run on the NanoSight instrument. Nanoparticle Tracking Analysis tracked particles between 10-2000 nm in diameter for 749 frames to yield these results.